Structure of Subnucleosomal Particles. Tetrameric $(H3/H4)_2$ 146 Base Pair DNA and Hexameric $(H3/H4)_2(H2A/H2B)_1$ 146 Base Pair DNA Complexes†

Christopher M. Read,* John P. Baldwin, and Colyn Crane-Robinson
Biophysics Laboratories, Portsmouth Polytechnic, Portsmouth PO1 2DT, U.K.
Received September 10, 1984; Revised Manuscript Received March 1, 1985

ABSTRACT: The tetrameric $(H3/H4)_2$ 146 base pair (bp) DNA and hexameric $(H3/H4)_2(H2A/H2B)_1$ 146 bp DNA subnucleosomal particles have been prepared by depletion of chicken erythrocyte core particles using 3 or 4 M urea, 250 mM sodium chloride, and a cation-exchange resin. The particles have been characterized by cross-linking and sedimentation equilibrium. The structures of the particles, particularly the tetrameric, have been studied by sedimentation velocity, low-angle neutron scattering, circular dichroism, optical melting, and nuclease digestion with DNase I, micrococcal nuclease, and exonuclease III. It is concluded that since the radius of gyration of the DNA in the tetramer particle and its maximum dimension are very close to those of the core particle, no expansion occurs on removal of all the H2A and H2B. Nuclease digestion results indicate that histones H3/H4 in the tetramer particle protect a total of 70 bp of DNA that are centrally located within the 146 bp. Within the 70 bp DNA length, the two terminal regions of 10 bp are, however, not strongly protected from digestion. The optical melting profile of both particles can be resolved into three components and is consistent with the model of histone protection of DNA proposed from nuclease digestion. The structure proposed for the tetrameric histone complex bound to DNA is that of a compact particle containing 1.75 superhelical turns of DNA, in which the H3 and H4 histone location is the same as found for the core particle in chromatin by histone/DNA cross-linking [Shick, V. V., Belyavsky, A. V., Bavykin, S. G., & Mirzabekov, A. D. (1980) *J. Mol. Biol. 139*, 491–517]. Optical melting of the hexamer particle shows that each $(H2A/H2B)_1$ dimer of the core particle protects about 22 base pairs of DNA.

Reconstitution of various histone mixtures with DNA have previously shown that H3 + H4 could generate many of the properties of intact chromatin. Low-angle X-ray diffraction maxima characteristic of chromatin at 5.5, 3.5, and 2.7 nm were obtained with the arginine-rich pair alone (Boseley et al., 1976; Moss et al., 1977), and digestion of the complex with nucleases gave rise to DNA fragments also characteristic of those from chromatin (Camerini-Otero et al., 1976; Sollner-Webb et al., 1976). Furthermore, the arginine-rich histone pair was shown to be capable of inducing beadlike particles in the electron microscope (Bina-Stein & Simpson, 1977; Bina-Stein, 1978; Oudet et al., 1978) and inducing supercoiling in closed circular DNA (Camerini-Otero & Felsenfeld, 1977; Bina-Stein & Simpson, 1977). While these studies demonstrated the central role played by H3 and H4 in supercoiling the DNA, as originally proposed by Kornberg (1974), it became apparent that two types of particle were readily formed by reconstitution of H3 and H4, whether onto long DNA or onto core particle size DNA fragments. Both Simon et al. (1978) and Stockley & Thomas (1979) demonstrated that particles containing either tetrameric $(H3/H4)_2$ or octameric $(H3/H4)_4$ arginine-rich histones could be generated. The former authors used reconstitution onto core particle length DNA, and the latter used depletion of histones H2A/H2B from core particles in 1 M NaCl. The sedimentation coefficient of the octamer particle was given as 10.4 S by Simon et al. (1978) and as 9.1 S by Stockley & Thomas (1979), but that of the tetramer particle was given as 7.5 and 6.0 S, respectively. Since the *s* value and the histone/DNA ratio of the octamer particle were much the same as that of the core particle, it was concluded that this particle is compact like the core particle. The large reduction in the *s* value for the tetramer particle, relative to octamer, was taken by Simon et al. (1978) and by Stockley & Thomas (1979) to mean that the tetramer complex is not a compact particle. This view was supported by Klevan et al. (1978), who also reconstituted the arginine-rich histones onto core particle length DNA and used electric dichroism to investigate the tetramer particle produced. They concluded that the complex was very extended and contained 1.5 superhelical DNA turns.

In a detailed electron microscopy study of reconstitutes prepared from H3 + H4 and supercoiled DNA at various histone/DNA ratios, Thomas & Oudet (1979) concluded that while both tetramer and octamer complexes were produced, both products were beadlike with a diameter of 8.0–9.0 nm, contained core particle length DNA and compacted the DNA in a manner similar to the octameric complex of all four core histones in the nucleosome.

There is thus uncertainty as to whether a single $(H3/H4)_2$ tetramer can induce the formation of just one superhelical turn of DNA, as could be inferred from protection of DNA lengths only up to 70 nucleotides against deoxyribonuclease (DNase)[1] I (Stockley & Thomas, 1979), or is capable of supporting the full 1.75 superhelical turns found in the core particle as suggested by electron microscopy (Thomas & Oudet, 1979). Resolution of this problem should aid clarification of the details of nucleosome assembly and contribute to an understanding of the differing roles of the core histones in chromatin structure.

† This research was supported by the SERC of Great Britain.

[1] Abbreviations: DNase, deoxyribonuclease; TBE, 90 mM Tris–borate and 2.5 mM Na_2EDTA (pH 8.3); Tris, tris(hydroxymethyl)aminomethane; Na_2EDTA, disodium ethylenediaminetetraacetate; DTT, dithiothreitol; SDS, sodium dodecyl sulfate; PMSF, phenylmethanesulfonyl fluoride; CD, circular dichroism; bp, base pair; Exo III, exonuclease III.

0006-2960/85/0424-4435$01.50/0

The present work uses depletion of histones H2A and H2B from core particles under fairly mild conditions to produce homogeneous products that have been characterized as tetrameric $(H3/H4)_2$ 146 bp DNA and as hexameric $(H3/H4)_2(H2A/H2B)_1$ 146 bp DNA. Depletion of H2A and H2B was achieved by using conditions very similar to those of Sibbet & Carpenter (1983) for which lack of H3 and H4 exchange between particles was clearly established. The production of octamer $(H3/H4)_4$ 146 bp DNA particles was therefore largely avoided. The depleted particles have been studied in detail by nuclease digestion and by a variety of physical methods. It is concluded that the tetramer particle is similar in overall dimensions to the core particle and is one in which the $(H3/H4)_2$ tetramer is bound to the central 70 base pairs of DNA, in addition to binding to a stretch of DNA of unknown length at the ends of the particle.

Materials and Methods

Preparation of Core Particles. Core particles were prepared by micrococcal nuclease digestion of chicken erythrocyte nuclei essentially as described by Suau et al. (1977). Following zonal centrifugation, fractions containing cosedimenting core particles and chromatosomes were collected, sucrose was removed by dialysis, and chromatosomes were precipitated from the mixture by the addition of sodium chloride to 150 mM (Olins et al., 1976). Core particles that remained in solution were shown by gel electrophoresis to contain all four core histones but no histone H1 and H5. The majority of the DNA was 146 bp in length, though about 10% was 167 bp in size and arose from an inability to remove histone H1/H5-depleted chromatosomes (Sollner-Webb et al., 1978).

Histone H2A/H2B Depletion of Core Particles. Core particles in 10 mM Tris-HCl, 2 mM Na_2EDTA, 1 mM cacodylic acid, and 1 mM PMSF (pH 7.4) were made 250 mM in sodium chloride and either 3 or 4 M in urea by the addition of buffered stock solutions of 4 M sodium chloride and 8 M urea (deionized), so diluting to 2.5 mg/mL DNA. A quarter volume of packed equilibrated resin AG 50W-X2 (Na^+ form; Bio-Rad) was added to this solution to start depletion, and the mixture was then continuously rolled at 4 °C for 2 h. Resin was spun down by centrifugation at 12000*g* for 1 min and the supernatant removed and extensively dialyzed against 10 mM Tris-HCl, 2 mM Na_2EDTA, 1 mM cacodylic acid, and 1 mM PMSF (pH 7.4). The dialyzed solution containing the depleted particles was layered onto 5–20% exponential sucrose density gradients prepared in the above buffer and centrifuged at 5 °C for 24 h at 284000*g* in an MSE 6 × 14 mL swing-out rotor. Gradients were fractionated by pumping Maxidens (1.90 g/mL; Nyegaard) into the bottom of the tubes. The outflow passed through a UV monitor absorbing at 254 nm (Isco), containing a turbulent-free flow cell, and then into a fraction collector.

Cross-Linking. Chemical cross-linking of histones in core particles, in the 7.2S and 9.2S particles (at 0.1 mg/mL DNA), was achieved with 3 mg/mL dimethyl suberimidate (a gift from Dr. J. O. Thomas) in 137 mM sodium borate buffer (pH 9.0), essentially as described previously (Thomas & Kornberg, 1978; Stockley & Thomas, 1979; Thomas & Oudet, 1979). Samples containing the products of cross-linking were analyzed on 5% polyacrylamide slab gels in 0.1% SDS and 100 mM sodium phosphate, pH 7.2 (Weber & Osborn, 1969).

Nuclease Digestion of Unlabeled Particles. Native core particles and $(H3/H4)_2$ 146 bp DNA particles (at 0.5 mg/mL DNA) in 50 mM Tris-HCl, 1.2 mM magnesium chloride, 1 mM cacodylic acid, 1 mM PMSF, and 0.2 mM Na_2EDTA (pH 8.0) were incubated at 37 °C with either 20 units of DNase I/mg of DNA (Sigma Chemical Co.) or 50 units of exonuclease III/mg of DNA (Bethesda Research Laboratories). Aliquots were removed at intervals, and digestion was terminated by the addition of 100 mM Na_2EDTA to give a final concentration of 10 mM. Micrococcal nuclease digestions were performed as above, except that magnesium chloride was replaced with calcium chloride and that 40 units of micrococcal nuclease/mg of DNA (MRE, Porton Down) was used.

5′ End Labeling. Core particles and $(H3/H4)_2$ 146 bp DNA particles were labeled at their 5′ DNA termini by incubation for 1 h at 37 °C with 95 μM [γ-^{32}P]ATP [42 Ci/mmol; prepared by the method of Maxam & Gilbert (1977); a gift from Dr. T. Moss], and 2 units of T4 polynucleotide kinase (Miles) in a buffer containing 50 mM Tris-HCl, 4 mM DTT, 1.2 mM magnesium chloride, and 0.2 mM Na_2EDTA (pH 8.0). The final concentration of particles was 0.4 mg/mL DNA in a total volume of 20 μL. Typically, the incorporation of ^{32}P into 5% trichloroacetic acid insoluble material was found to be about 1.30 phosphates per core particle and 1.50 phosphates per $(H3/H4)_2$ 146 bp DNA particle.

Nuclease Digestion of End-Labeled Particles. Micrococcal nuclease digestion of end-labeled $(H3/H4)_2$ 146 bp DNA particles was initiated by adding to the incubated solution of labeled particles a 20 μL volume containing 0.32 unit of micrococcal nuclease (MRE, Porton Down) in 50 mM Tris-HCl, 4 mM DTT, 2.4 mM calcium chloride, and 0.2 mM Na_2EDTA (pH 8.0). Aliquots (5 μL) were removed at intervals, and digestion was terminated by adding 2.5 μL of a solution of 30 mM Na_2EDTA and 300 μg/mL proteinase K (Boehringer). Incubation at 37 °C continued for another hour, after which the sample was diluted to 40 μL with 8 M urea, 9 mM Tris–borate, 0.25 mM Na_2EDTA, 0.02% bromophenol blue, and 0.02% xylene cyanol FF (pH 8.3). Samples were denatured by boiling for 5 min immediately prior to loading on an 8% polyacrylamide–7 M urea TBE slab gel (Lutter, 1979). Gels were autoradiographed with Kodak No-screen X-ray film at −20 °C.

DNase I digestion of end-labeled core particles was performed similarly by adding a 20 μL volume containing 0.16 unit of DNase I (Sigma Chemical Co.) in 50 mM Tris-HCl, 4 mM DTT, 1.2 mM magnesium chloride, and 0.2 mM Na_2EDTA (pH 8.0) to the incubated and kinased particles.

Gel Electrophoresis. Analysis of histones was carried out on discontinuous 12% polyacrylamide–0.1% SDS slab gels (Laemmli and Favre, 1973). Gels were stained by immersion in 0.03% Coomassie Blue R250 (Pierce) in 25% ethanol, 10% acetic acid, and 65% water.

DNA fragments were electrophoresed under denaturing conditions on 12% polyacrylamide–7 M urea TBE slab gels (Maniatis et al., 1975). Samples were prepared by incubation with 100 μg/mL proteinase K (Boehringer) for 1 h at 37 °C followed by two chloroform/isoamyl alcohol (24:1) extractions and precipitation of DNA with 4 volumes of ethanol at −20 °C. DNA was collected by centrifugation at 12000*g* for 15 min and the pellet washed with 1:1 ethanol–diethyl ether and centrifuged again for 10 min. The dried pellets were redissolved in 8 M urea, 9 mM Tris–borate, 0.25 mM Na_2EDTA, 0.02% bromophenol blue, and 0.02% xylene cyanol FF (pH 8.3) and then denatured by boiling for 5 min immediately before loading on the gel. Gels were stained with 1 μg/mL ethidium bromide solution, and DNA was visualized by short wavelength UV transillumination.

Histone–DNA complexes were electrophoresed on 8% polyacrylamide TBE slab gels (Maniatis et al., 1975). Gels were stained for DNA with ethidium bromide and then subsequently

stained for protein with Coomassie Blue R250 (Pierce) in order to distinguish histone–DNA complexes from histone-free DNA.

Two-dimensional gel electrophoresis was as follows: electrophoresis of particles (as described above) was carried out in the first dimension, staining only for DNA. The band containing particles was visualized by short wavelength UV transillumination and excised with a scalpel. The gel slice was soaked in 50 mM Tris-HCl and 3% SDS (pH 6.8) for 30 min and set into the stacking gel of an SDS–polyacrylamide discontinuous slab gel, such that the direction of electrophoresis was perpendicular to the first. The gel was then stained for protein with Coomassie Blue R250.

Densitometer traces were obtained from photographic negatives of gels by using a Vitratron TLD 100 scanner.

Circular Dichroism. CD spectra of particles, dialyzed into 5 mM sodium phosphate buffer (pH 7.2), were recorded on a Cary 61 spectropolarimeter. DNA concentrations were determined from the absorbance at 260 nm. CD difference spectra (particle − 146 bp DNA) were converted from ellipticities expressed in units of deg cm^2 (dmol of phosphate)$^{-1}$ to units of deg cm^2 (dmol of amino acid)$^{-1}$ assuming 3.36, 2.49, and 1.62 mol of amino acid/mol of phosphate for core, hexamer, and tetramer particles, respectively. Histone secondary structure content was estimated by curve fitting to the α-helix and β-sheet spectra of Chen et al. (1974) and to a random coil spectrum obtained from an equimolar mixture of the core histones in 8 M urea. Helicity was also estimated from the ellipticity at 222 nm assuming no β-sheet, a helical ellipticity of −30 000, and a random coil ellipticity of −1048 deg cm^2 (dmol of amino acid)$^{-1}$ (Moss et al., 1976).

Thermal Denaturation. Samples were prepared by dialysis for 48 h against 0.25 mM EDTA (pH 7.0). Denaturation was monitored at 260 nm in stoppered 1-cm path-length quartz cuvettes on a Perkin-Elmer 472 spectrophotometer fitted with jacketed cell holders containing water circulating from a thermostated water bath. Temperatures were recorded with a platinum resistance thermometer placed in a dummy 1-cm quartz cuvette adjacent to the sample cell. The rate of increase in temperature was 1 °C/min. The change in absorbance with temperature was continuously monitored on an X-Y plotter, and derivative curves were obtained from data sampled at 1 °C intervals. Derivative melting profiles were resolved into component transitions by fitting the envelope to two or three Gaussian curves.

Sedimentation. Sedimentation coefficients of particles separated in preparative sucrose density gradients were determined by the method of Funding & Steensgaard (1973), modified to account for centrifugation in swing-out rotors.

Velocity sedimentation and low-speed equilibrium sedimentation experiments were performed on a MSE Centriscan 75 ultracentrifuge equipped with scanning double-beam UV absorption optics at 254 nm. Velocity sedimentation was carried out at 35 000 rpm, 20 °C. Sedimentation coefficients were calculated from the slope of the straight line, fitted by linear regression, of a plot of the natural logarithm of the radius at the midpoint of the moving boundary vs. time. These were corrected to standard conditions to yield $s_{20,w}$ values. Low-speed equilibrium sedimentation data were obtained for particles at 4700 rpm, 5 °C, after overspeeding at 7500 rpm for 3 h. An equilibrium gradient was attained when scans taken 12 h apart were identical. The latter trace was taken to show the equilibrium distribution. A base line for measurement of concentrations was obtained by sedimenting the particles completely and scanning again at 4700 rpm.

Neutron Scattering. Low-angle neutron scattering studies were performed at the Institute Max von Laue-Paul Langevin, Grenoble, using instrument D11 (Schmatz et al., 1974; Ibel, 1976). To carry out contrast variation measurements, samples of core particles and $(H3/H4)_2$ 146 bp DNA complexes were dialyzed against 10 mM Tris-HCl, 2 mM Na_2EDTA, 1 mM cacodylic acid, and 1 mM PMSF (pH 7.4) having different H_2O/D_2O ratios. The samples in 0.1-cm path-length quartz cuvettes were measured at two sample-to-detector distances, normally 2.53 and 0.84 m, to give low-angle neutron scatter curves in the interval of k [=sin (θ/λ), where 2θ is the scatter angle and λ is the wavelength (0.8 nm)] between 0.18 and 3.25 nm^{-1}. Curves were merged by using the overlapping regions and corrected to differential scattering cross sections per gram of DNA $[4\pi N_0 S(k,\bar{\rho})/M_{DNA}]$, according to Suau et al. (1977). $S(k,\bar{\rho})$ is the differential scattering cross section for a particular value of k at contrast $\bar{\rho}$. M_{DNA} is the molecular weight of the DNA. The radius of gyration R_g was measured at different contrasts, from the slope of the line fitted by linear regression, on a plot of ln $[4\pi N_0 S(k,\bar{\rho})/M_{DNA}]$ vs. k^2 (the Guinier plot). Linear plots were obtained with correlation coefficients greater than 0.98 in the region where the Guinier approximation holds ($k < 0.625$ nm^{-1} at high contrast). For the tetramer particle in 40% D_2O, close to its contrast matched position, the correlation coefficient was 0.74. Zero-angle differential scattering cross sections, at various contrasts, were obtained by extrapolation of the low-angle curves using the Guinier plot. These were converted to the differential scattering cross sections per particle, $S(0,\bar{\rho})$, since the molecular weight of the DNA in the particles was well characterized by gel electrophoresis.

The distance distribution functions, $D(u)$, of the particles were determined by inverse Fourier transformation of the full scatter curves obtained in 100% D_2O. In practice, since the curves extend over a finite interval of k, the low-angle region was extrapolated to zero angle by using the Guinier relation and the high-angle region extended to zero intensity with a k^{-4} approximation. The data points were subsequently interpolated to yield k values of equal spacing, and integration was performed according to Simpson's rule.

Results and Discussion

Nucleosome core particles, from chicken erythrocyte nuclei, were selectively depleted in histones H2A and H2B by using 3 M urea and 250 mM NaCl in the presence of the cation-exchange resin AG 50W-X2, as described under Materials and Methods. The products of depletion were separated on sucrose gradients at low ionic strength and in the absence of urea. Figure 1 shows that four major products can be defined which have $s_{20,w}$ values of 5.2, 7.2, 9.2, and 11.3 S.

SDS gel electrophoresis was used initially to aid assignment of the peaks, by loading in each slot a defined amount of DNA (Figure 2). The 5.2S peak contained no protein and is clearly free DNA of core particle length. The 11.3S peak is undepleted core particles and is used as a standard (lanes 3, 6, and 9). The 7.2S peak (lanes 1, 4, and 7) contains only histones H3 and H4, and comparison with core particles at the same DNA loading (for three different loadings) suggests that the amount of these histones is present relative to DNA as in core particles; i.e., the 7.2S particles contain the tetrameric histone complex, $(H3/H4)_2$, bound to the 146 bp DNA. By the same token the 9.2S particles contain H2A and H2B in addition to the $(H3/H4)_2$ tetramer, but by comparison with core particles, some H2A and H2B have been lost. Bearing in mind the ease with which a single $(H2A/H2B)_1$ dimer is lost from the core histone octamer protein (Thomas & Kornberg, 1975a,b; Eickbush & Moudrianakis, 1978; Ruiz-Carrillo & Jorcano,

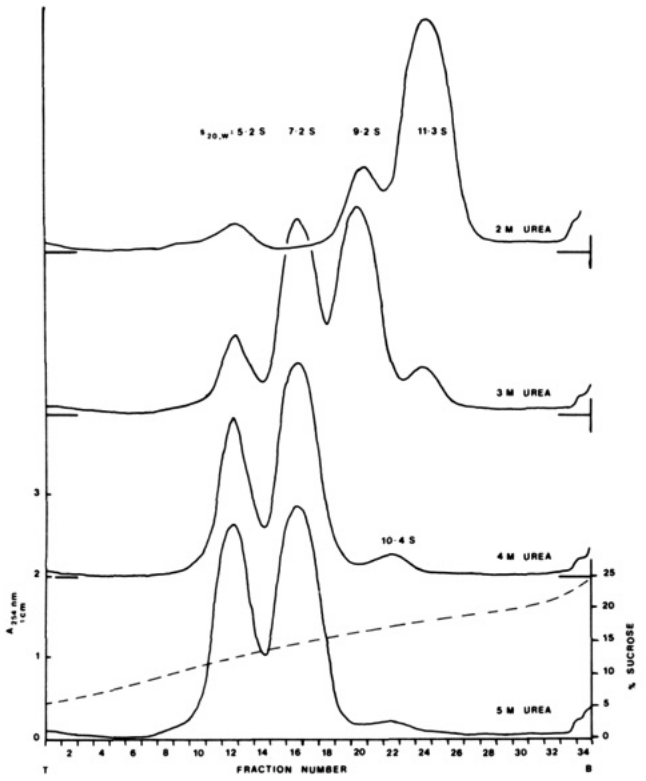

FIGURE 1: Rate zonal sedimentation profiles in 10 mM Tris-HCl, 2 mM Na_2EDTA, 1 mM cacodylic acid, and 1 mM PMSF (pH 7.4) showing the separation of complexes produced by core particle depletion in 250 mM NaCl and 2–5 M urea at 10 mg of DNA/mL of resin AG 50W-X2 for 2 h. T = top and B = bottom of gradients.

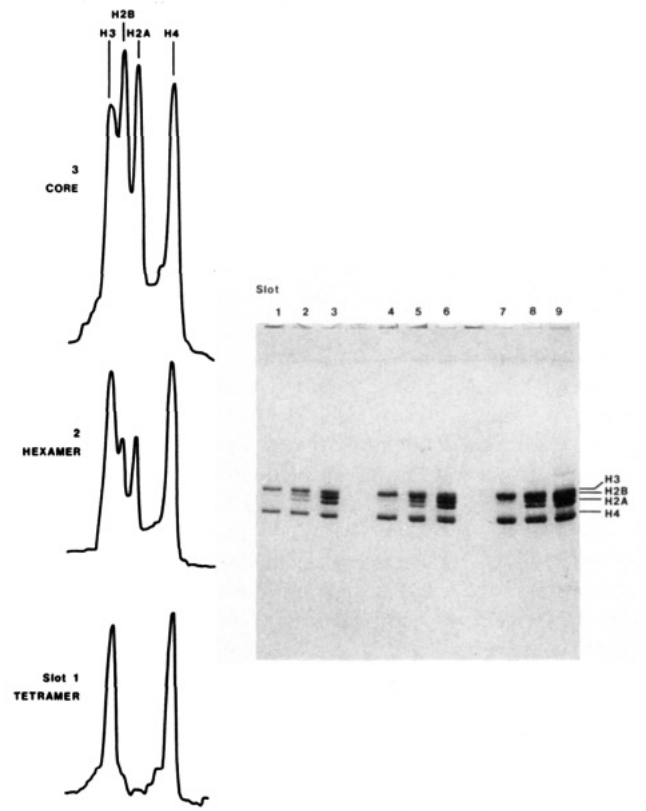

FIGURE 2: (Right) SDS–polyacrylamide gel of proteins from particles separated by the sucrose gradient of Figure 1. Histones from the 7.2S peak (slots 1, 4, and 7), the 9.2S peak (slots 2, 5, and 8), and the 11.3S peak (slots 3, 6, and 9) at loadings of 2, 4, and 8 μg of DNA per lane (left to right). (Left) Densitometer tracings of slots 1–3.

1979; Godfrey et al., 1980; Philip et al., 1980), the 9.2S particle could contain the hexameric histone complex $(H3/H4)_2$-$(H2A/H2B)_1$ bound to the 146 bp DNA.

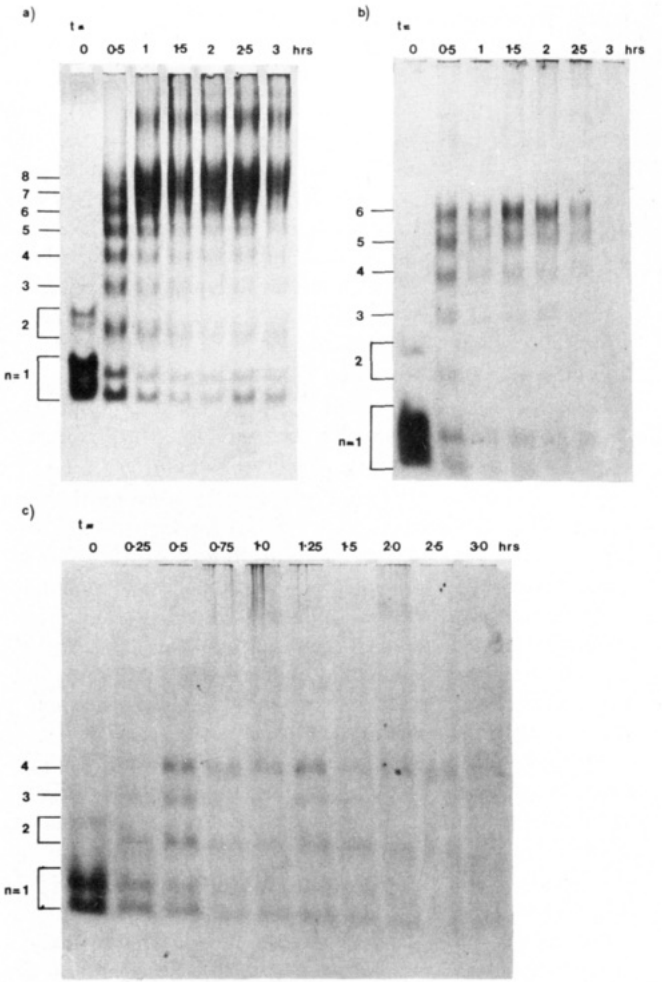

FIGURE 3: Time course of histone–histone cross-linking with dimethyl suberimidate for (a) core particles, 11.3S peak, (b) the 9.2S particles, (c) the 7.2S particles. Analysis on a 5% polyacrylamide–SDS–phosphate gel.

Depletion of core particles under the stronger conditions of 4 or 5 M urea gives rise to a small component of 10.4S in the sucrose gradients (Figure 1). SDS gel electrophoresis indicated that it contained only H3 and H4 (not shown). This is presumably the particle containing the octamer $(H3/H4)_4$ bound to core particle DNA that was characterized by Simon et al. (1979). It was not studied further, since only low amounts were produced by the depletion method used here, as expected for a product of rearrangement.

Characterization of 7.2S and 9.2S Particles. (*1*) *Cross-Linking.* To better define the histone composition of the 7.2S and 9.2S particles, they were chemically cross-linked at pH 9.0 with dimethyl suberimidate and the products compared with those from core particles.

Figure 3 shows the time course of this cross-linking. As expected, core particles (the 11.3S peak from the gradient; Figure 3a) show a set of bands up to an octamer, with indication of a larger product at longer times that is presumably a 16-mer (Stein, 1979). The 9.2S particle (Figure 3b) shows a set of bands up to a hexamer with very little higher molecular weight material. This implies a hexameric protein composition for this particle. Cross-linking of the 7.2S particle (Figure 3c) gives a set of bands up to a tetramer, indicating that this particle has a tetrameric histone content.

(*2*) *Gel Electrophoresis.* A further characterization of the products of depletion was carried out on "particle" gels. Figure 4 shows such a gel, stained for DNA and subsequently for

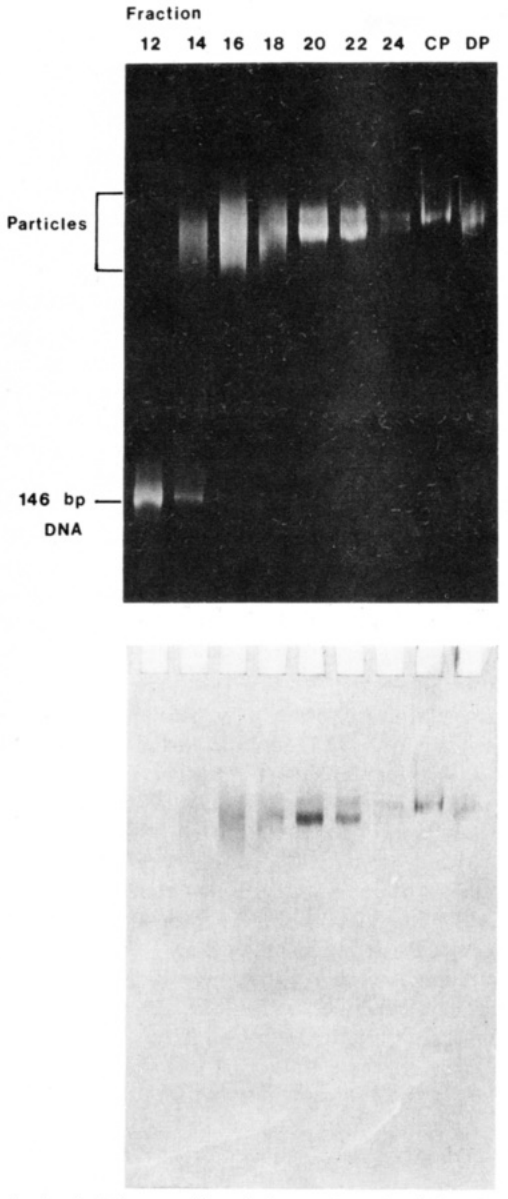

FIGURE 4: Analysis by particle gel electrophoresis of fractions from the gradient of Figure 1. Gel stained with ethidium bromide (top) and then with Coomassie blue (bottom). CP, core particles. DP, unseparated products of depletion.

protein, of several fractions from the sucrose gradient given in Figure 1. Fraction 12 is the 5.2S peak and is seen to be free DNA, as expected. Fraction 24 is the 11.3S peak and shows a double band, the upper of which runs identically with control, undepleted core particles. Fraction 20, the 9.2S particle, also exhibits two bands, the faster of which is much the more strongly staining both for DNA and for protein. There is therefore some cross-contamination between fractions 20 and 24.

The 7.2S particle (fraction 16) runs as an ill-defined band in this gel system. Considering the apparently well-defined nature of the 7.2S particle, the width of the band from the 7.2S particles is surprising. A possible explanation is that the 7.2S fraction actually contains a range of histone composition that is readily revealed by the particle gel, but not by the other techniques so far described. Proteins were therefore run out of particle bands by soaking in SDS and electrophoresing in a second dimension containing 0.1% SDS. Figure 5 shows a comparison of the proteins so extracted from the core particle control and from the 7.2S particle of Figure 4. Whereas the core particle shows the usual four histones, the 7.2S particle

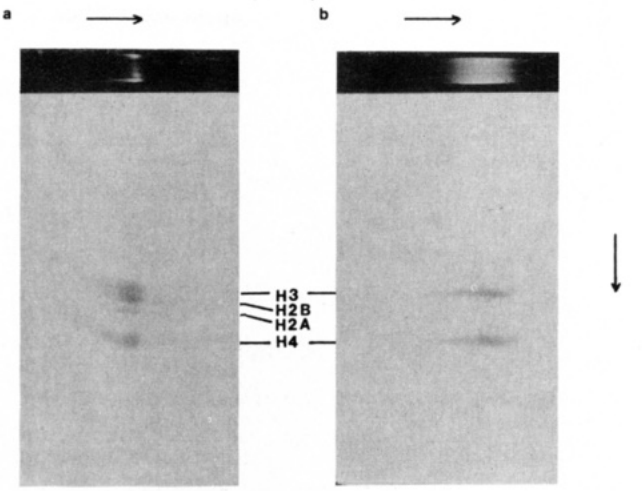

FIGURE 5: Two-dimensional gel electrophoresis of core particles (a) and the 7.2S particles (b). The bands were cut out from the first-dimension particle gel (stained for DNA) and then run in the second dimension on a 0.1% SDS–12% polyacrylamide slab gel.

shows only H3 and H4 all the way across the band, as expected from the electrophoresis of the total protein shown in Figure 2. More importantly, the intensity of Coomassie staining of H3 relative to H4 is the same (about 1:1) across the 7.2S particle band. The profile of ethidium bromide staining in the first dimension direction of the particle gel is also mirrored by the intensity of Coomassie blue staining in the same direction in the SDS gel, and this implies a constant histone/DNA ratio across the particle band. A fraction from the center of a sucrose gradient peak, e.g., fraction 16, might nevertheless contain a range of particles. However, fractions from the leading and trailing edges of the 7.2S peak (fractions 18 and 14, respectively) also exhibit a particle band of similar width to that of fraction 16. There is thus no evidence that the broad band in the particle gel of the 7.2S peak is due either to variations in relative histone composition or to variations in histone/DNA ratio.

(*3*) ***Sedimentation Equilibrium.*** Low-speed equilibrium runs were carried out for control core particles and for the 9.2S and 7.2S particles in 10 mM Tris-HCl, 5 mM Na_2EDTA, 1 mM cacodylic acid, and 1 mM PMSF, pH 7.4 (see Materials and Methods). The slope of ln c (particle concentration) vs. r^2 plots is $M_r(1 - v_2\rho_0)$, where M_r is the apparent molecular weight, v_2 the partial specific volume of the macromolecule, and ρ_0 is the solvent density. Since the partial specific volume of the particles is not known experimentally, their molecular weight cannot be calculated directly. The data were therefore treated as follows: the product $M_r(1 - v_2\rho_0)$ was calculated for particles of various compositions by using the data for v_2 of amino acids from Cohn & Edsall (1943) and takine v_2 for histone-free DNA as 0.550 mL/g (Cohen & Eisenberg, 1968). The values so calculated were compared with those determined experimentally. For core particles the calculated partial specific volume is 0.652 mL/g, while the value measured by Zama et al. (1978) was 0.670 mL/g. It was therefore assumed that the calculated partial specific volumes of all the particles were 3% too low, and they were therefore increased by this amount when the product $M_r(1 - v_2\rho_0)$ was calculated. Table I shows these calculated products for (H3/H4) DNA particles and for particles containing all four histones. The experimental value for the 7.2S particle of 53 786 daltons fits best to the tetrameric complex $(H3/H4)_2$ 146 bp DNA, whereas the experimental value of 60 271 daltons for the 9.2S particle fits best to the hexameric complex $(H3/H4)_2(H2A/H2B)_1$ 146 bp DNA. These results support the previous assignments of

Table I: Calculated Products for (H3/H4)-DNA Particles and for Particles Containing All Four Histones

composition of particle	M_r	partial sp vol, v_2 (mL/g)	$M_r(1 - v_2\rho_0)$
7.2S particles			53 786[a]
$(H3/H4)_1$(146 bp DNA)$_1$	122 966	0.607	48 210
$(H3/H4)_2$(146 bp DNA)$_1$	149 572	0.635	54 587
$(H3/H4)_3$(146 bp DNA)$_1$	176 178	0.653	60 964
$(H3/H4)_4$(146 bp DNA)$_1$	202 784	0.667	67 341
9.2S particles			60 271[a]
$(H3/H4)_1(H2A/H2B)_1$-(146 bp DNA)$_1$	150 700	0.636	54 690
$(H3/H4)_2(H2A/H2B)_1$-(146 bp DNA)$_1$	177 306	0.655	61 068
$(H3/H4)_2(H2A/H2B)_2$-(146 bp DNA)$_1$	205 040	0.670	67 498

[a] Observed values of $\bar{M}_{r,app}(1 - v_2\rho_0)$ obtained from low-speed sedimentation equilibrium.

the 7.2S and 9.2S particles, respectively, to tetrameric and hexameric histone complexes with 146 bp of DNA.

Structure and Conformation of the Tetrameric and Hexameric Particles. (1) Sedimentation Velocity. This method is potentially capable of giving information on overall shape, and so values of $s_{20,w}$ were obtained in the analytical ultracentrifuge for core particles, for 9.2S and 7.2S particles, and for free 146 bp DNA in 10 mM Tris-HCl, 2 mM Na_2EDTA, 1 mM cacodylic acid, and 1 mM PMSF (pH 7.4). The values obtained were 10.85, 9.08, 6.82, and 5.11 S at a concentration of 40–50 μg of DNA/mL. These s values were converted to frictional coefficients, f_{obsd}, by using the values for $M_r(1 - v_2\rho_0)$ given in Table I and then into frictional ratios $(f/f_0)_{obsd}$ by calculating the frictional coefficient f_0 of the unhydrated equivalent spheres of nucleoprotein. Table II shows these values. These frictional ratios can then be interpreted as the product of a frictional ratio due to solvation and a frictional ratio due to shape. Since the core particle is approximately a cylinder of height 5.7 nm and diameter 11.0 nm (Finch et al., 1977, 1980, 1981; Bentley et al., 1981), then $(f/f_0)_{shape}$ might be taken as that for an oblate ellipsoid of revolution of axial ratio 2, i.e., $(f/f_0)_{shape} = 1.042$. The frictional ratios due to solvation can then be converted into grams of water bound per gram of particle. The solvation levels obtained are unrealistically high, e.g., 4.6 g of water/g of particle for the tetramer particle. Such high solvation values result from high frictional ratios which in turn are due to the use of the low f_0 values derived from the volumes of the "dry" particles. The volume is 228 nm^3 for the core particle, although the volume of a cylinder of the above dimensions is 542 nm^3. A more realistic model is thus to treat the core particle as a flat cylinder of the above dimensions, for which $f_0 = 1.021 \times 10^{-7}$ g s^{-1} (Eisenberg & Felsenfeld, 1981). Table II gives values of $(f/f_0)_{obsd}$ calculated for all three particles by using this value of f_0, on the assumption (based on the present results; see below) that all the particles have essentially the same shape. The core particle frictional ratio is close to unity (1.0163), implying very little external hydration, as noted by Eisenberg & Felsenfeld (1981). If the core particle frictional ratio of 1.0163 is taken as the shape contribution for the other two particles, their external hydration can be calculated in the usual way, and this is also given in Table II. The external water of hydration in the hexamer and tetramer particles is probably due to the exposure of additional lengths of DNA to the solvent on loss of histone.

(2) Small-Angle Neutron Scattering from Solutions of Tetramer and Core Particles. This experimental approach, involving contrast variation in D_2O/H_2O mixtures, can yield the following information: (a) From the extrapolated zero-angle scattering, the contrast matched position, the molecular weight, and the volume of the particles can be calculated. This serves to check the composition of the particles. (b) The radius of gyration at infinite contrast can be calculated to give overall shape information. (c) The limit of the distance distribution function yields the maximum dimension of the particle, also giving general shape information. (d) The form of the observed distance distribution function can be compared to that calculated for model shapes, giving somewhat more detailed shape information.

Experimental scatter curves were obtained at four contrasts: 20, 31, 65, and 100% D_2O for core particles and at 0, 40, 65, and 100% D_2O for the tetramer particle. They were plotted as the logarithm of the differential scattering cross section per gram of DNA, $\ln [4\pi N_0 S(k,\bar{\rho})/M_{DNA}]$, vs. k^2, the square of the momentum transfer (the so-called Guinier plot). The differential scattering cross section at zero angle, $S(0,\bar{\rho})$, was obtained by extrapolation. Figure 6 shows $[S(0,\bar{\rho})]^{0.5}$ plotted vs. the solvent scattering length density, ρ_{sol}, for both particles. The intercepts on the ρ_{sol} axis give the contrast matched scattering length densities as $(2.74 \pm 0.01) \times 10^{10}$ cm^{-2} (47.5% D_2O) for the core particle and $(2.99 \pm 0.01) \times 10^{10}$ cm^{-2} (51.3% D_2O) for the tetramer particle. The value for core particles is in good agreement with that found by Suau et al. (1977). As expected the composition of the tetramer particle is toward the direction of the contrast matched position of histone-free DNA. The slopes of the $[S(0,\rho)]^{0.5}$ vs. ρ_{sol} plots give the apparent volumes, V_C, of the particles. These are the following: for core particles, $V_C = 200.5$ nm^3; for tetramer particles, $V_C = 134.9$ nm^3.

These apparent volumes are related to the dry volumes, V_F, by $V_C = V_F - V_E$, where the correction factor V_E $(=1 - \Omega_E)$ accounts for the exchange of deuterium for hydrogen. In order to obtain the dry volume V_F of the tetramer particle and so calculate its molecular weight, a value for V_E is required. Infrared studies of chromatin deuteration (Bradbury et al., 1962) showed that all hydrogens in the DNA base pairs exchange rapidly and that 40% of amide hydrogens in histones are hard to exchange. This figure can be assessed for the core

Table II: Summary of Hydrodynamic Data Obtained by Velocity Sedimentation

	core $(H3/H4)_2(H2A/H2B)_2$-(146 bp DNA)$_1$	hexamer $(H3/H4)_2(H2A/H2B)_1$-(146 bp DNA)$_1$	tetramer $(H3/H4)_2$-(146 bp DNA)$_1$
sedimentation coeff, $s_{20,w}$ (S)	10.85	9.08	6.82
frictional coeff, f ($\times 10^7$ g s^{-1})	1.038	1.122	1.333
obsd frictional ratio,[a] $(f/f_0)_{obsd}$	1.452	1.660	2.111
obsd frictional ratio,[b] $(f/f_0)_{obsd}$	1.016	1.098	1.306
solvation[c] (g of H_2O/g of particle)	0	0.172	0.711

[a] Using f_0 values of unhydrated equivalent spheres of the appropriate composition. [b] Assuming the value of $f_0 = 1.021 \times 10^{-7}$ g s^{-1} calculated for a solid cylinder of diameter 11.0 nm and height 5.7 nm (Eisenberg & Felsenfeld, 1981). [c] Calculated from $(f/f_0)_{obsd}$ in the line above and assuming the core particle fractional ratio due to shape, i.e., 1.016.

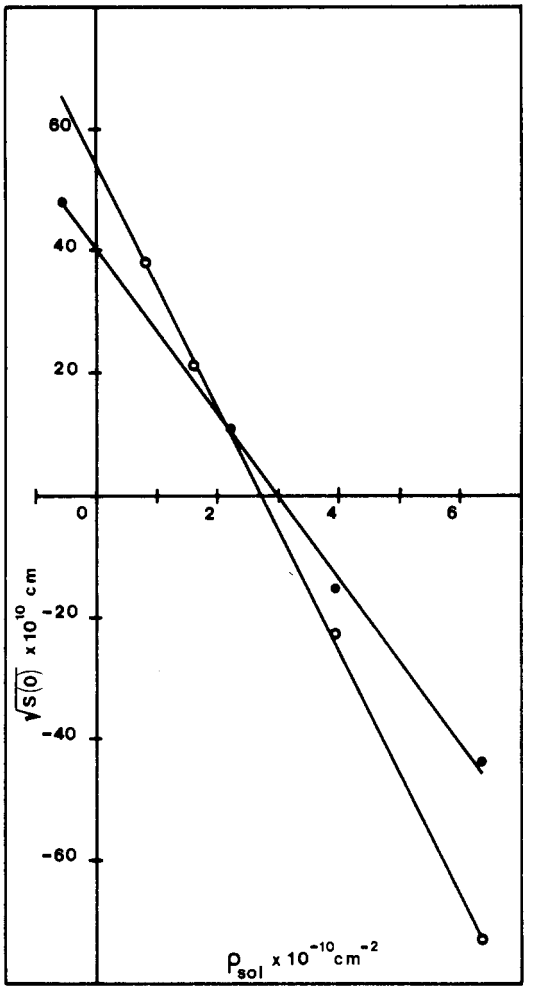

FIGURE 6: Plot of the square root of the differential scattering cross section at zero angle, $S(0,\bar{\rho})$, vs. the solvent scattering length density, ρ_{sol}, for core particles (○) and $(H3/H4)_2$ 146 bp DNA tetramer particles (●).

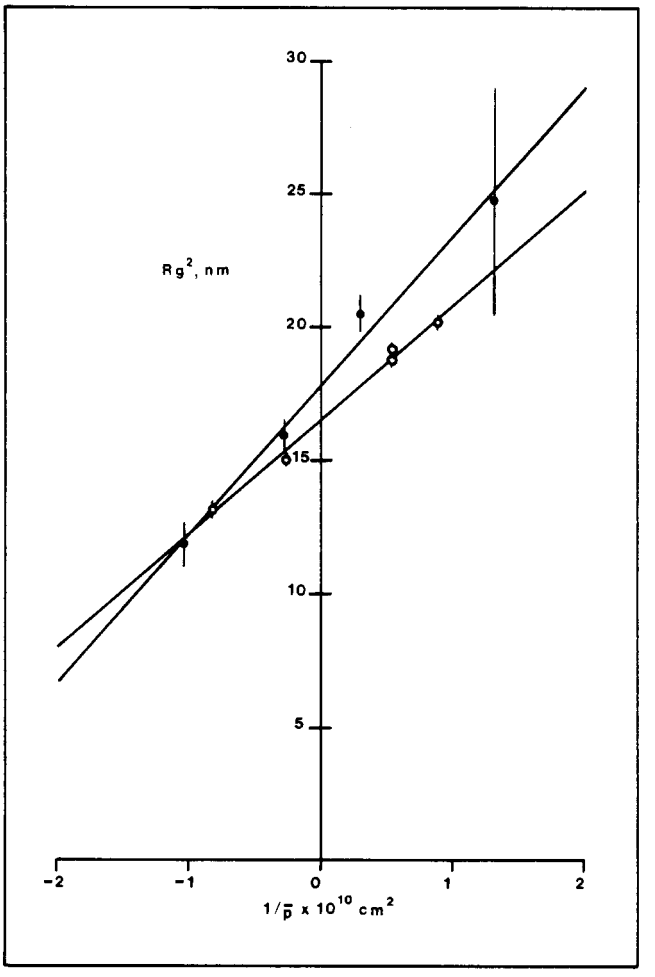

FIGURE 7: Ibel–Stuhrmann plot of the square of the observed radius of gyration, R_g, obtained from Guinier plots, vs. the reciprocal of the contrast, $1/\bar{\rho}$, for core particles (○) and $(H3/H4)_2$ 146 bp DNA tetramer particles (●).

particle since its composition is known. There are 2654 exchangeable hydrogens in all, of which 564 are in the DNA. Sixty percent of the remaining hydrogens in addition to these 564 makes a total, n, of 2261 that exchange. This gives a correction volume V_E = 34.1 nm^3, since $V_E = n(\Delta b/\Delta\rho)$ where Δb is the difference in the scattering length of deuterium and hydrogen and $\Delta\rho$ is the difference in the scattering length densities of D_2O and H_2O. The apparent volume V_C of the core particle is measured as 200.5 nm^3, and the dry volume V_F is calculated as 228.0 nm^3, assuming a molecular weight of 205 040 and a partial specific volume of 0.670 mL/g. So the observed correction volume V_E = 27.5 nm^3 is in fair agreement with that calculated assuming that only 40% of amide hydrogens are not exchanged. If this percentage is now applied to the tetramer particle, having 1608 total number of exchangeable hydrogens, only 190 remain unexchanged. This gives a value of V_E = 21.4 nm^3. The dry volume V_F is thus 134.9 + 21.4 = 156.3 nm^3, and this yields a molecular weight of 148 250, assuming a partial specific volume of 0.635 mL/g. The actual molecular weight of an $(H3/H4)_2$ 146 bp DNA particle is 149 572. Although an assumption of the composition of the tetramer particle has been made to calculate V_E (and the mass from V_F using the partial specific volume, v_2), the V_E term is only a small correction. If, for example, the 7.2S particle were initially taken to be the hexamer particle, $(H3/H4)_3$ 146 bp DNA, then, assuming 40% hard-to-exchange amide hydrogens, V_E = 27.8 nm^3. Hence, V_F = 162.7 nm^3, and the molecular weight would be 150 067. This is nevertheless very close to the actual molecular weight of the tetramer particle $(H3/H4)_2$ 146 bp DNA and not to that of the hexamer particle, which has a mass of 176 178 daltons. Thus, the apparent volume V_C observed for the 7.2S particle clearly shows it to have a mass corresponding to the tetramer particle, $(H3/H4)_2$ 146 bp DNA.

(*a*) *Contrast Dependence of the Radius of Gyration.* Guinier plots of the low-angle scattering data were used to obtain the radius of gyration at several contrasts. Figure 7 shows the Ibel–Stuhrmann plot of the measured radii of gyration vs. the reciprocal of the contrast. The intercept at $1/\bar{\rho}$ = 0 gives the radii of gyration at infinite contrast, R_C. For core particles, R_C was measured as 4.07 ± 0.02 nm. This is to be compared with published values of 3.94 ± 0.05 (Suau et al., 1977) and 4.11 ± 0.04 nm (Pardon et al., 1975). For the tetramer particle, R_C was measured as 4.24 ± 0.05 nm, and the similarity of this value to that for core particles immediately indicates that it is a compact particle. The slope of the Ibel–Stuhrmann plot gives the coefficient α. The positive values observed [(4.28 ± 0.19) × 10^{-4} for core particles and (5.63 ± 0.40) × 10^{-4} for the tetramer particle] show that the more strongly scattering components, the DNA in this case, are located toward the outside of the particles. The radii of gyration of the histone and DNA components can be separately assessed from the Guinier slopes at the contrast matched position of DNA and protein, respectively, i.e., at 65% and 40% D_2O. The measured values were as follows: for core

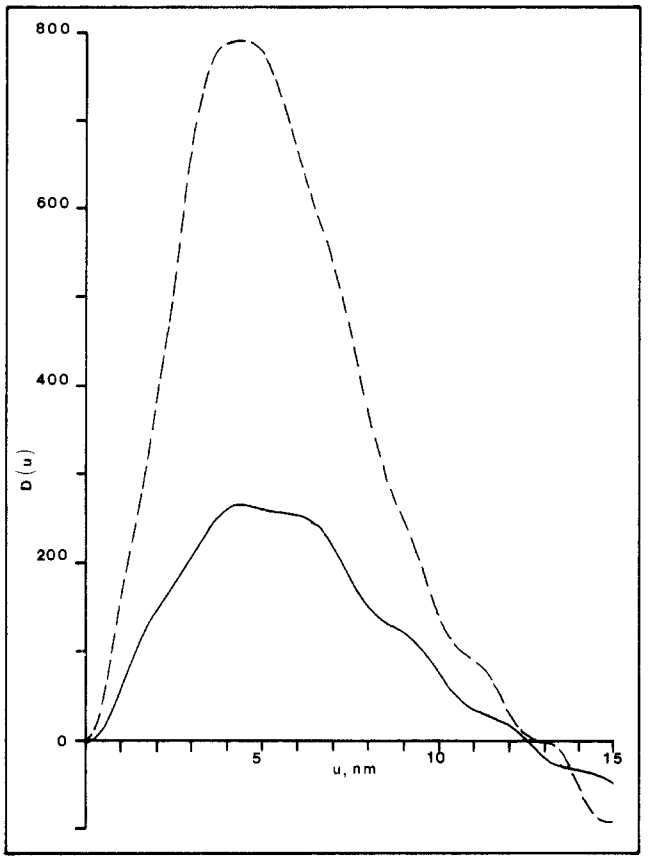

FIGURE 8: Distance distribution function $D(u)$ vs. chord length, u, for core particles (---) and $(H3/H4)_2$ 146 bp DNA tetramer particles (—) in 100% D_2O.

particles, R_g^{DNA} = 4.98 nm and $R_g^{protein}$ = 3.61 nm; for tetramer particles, R_g^{DNA} = 5.02 nm and $R_g^{protein}$ = 3.47 nm.

This indicates that the DNA conformation in the tetramer particle is very similar to that in core particles while the $(H3/H4)_2$ protein in the tetramer particle is at slightly lower radius than is the total protein of the core particle. This small difference between the particles is also reflected in the somewhat greater value of α for the tetramer particle. These results make it clear that the tetramer particle has essentially the same overall dimensions as the core particle, and any highly asymmetric shape such as proposed by Klevan et al. (1978) can be excluded.

(*b*) *Distance Distribution Function.* This function, $D(u)$, when measured at high contrast, e.g., in 100% D_2O, gives the number of chords, D, between scattering points as a function of the distance u between them and is therefore a one-dimensional representation of the distribution of length vectors within a particle. The function becomes zero at a value of u_{max} corresponding to the largest chord that can be drawn in the particle and reaches a maximum at a value of u ($u_{D(u)max}$) which is the most probable length of chord that can be drawn in the particle. Figure 8 shows this function for both core and tetramer particles in 100% D_2O. The area under the curves is not the same, principally because it is proportional to the square of the molecular mass:

$$\text{area} = \bar{\rho}^2 V_C^2 = \bar{\rho}^2(1 - \Omega_E)^2(M^2 v_2^2 / N_0^2)$$

Since all the factors on the right-hand side of this equation are known, the correctness of the inverse Fourier transform giving rise to the $D(u)$ function was checked for internal consistency by measurement of the area under the $D(u)$ vs. u curves. Figure 8 shows that the maximum chord length of the tetramer particle is 12.5 nm, very close to the value observed for core particles (12.75 nm). There is thus no evidence from this analysis that the tetramer particle has an expanded structure.

The shape of the observed distance distribution function can be used to obtain some idea of overall shape. Glatter (1979) has calculated the $D(u)$ function for some simple shapes such as spheres and prolate and oblate ellipsoids of revolution. The envelope shape of the $D(u)$ function differs in each case, and comparison with the experimental curve of Figure 8 shows that both core and tetramer particles are slightly oblate. A straightforward way of characterizing the shape is to calculate the value of the ratio $u_{D(u)max}/u_{max}$. This is 0.525 for spheres, but lower for ellipsoids. The value observed here for core particles was 0.33, while for the tetramer particle, it was 0.36. The tetramer particle, while clearly modeled by an oblate ellipsoid of revolution from the shape of the $D(u)$ curve, thus appears slightly more spherical than the core particle. The oblate or, more precisely, cylindrical shape of the core particle is well established from crystal structure analysis (Finch et al., 1977, 1980, 1981; Bentley et al., 1981). The simple interpretation of this study of the tetramer particle is that loss of the two $(H2A/H2B)_1$ dimers results in increased repulsions between the gyres of the DNA superhelix and thus a slight expansion in the direction of the axis of this superhelix but essentially no expansion at right angles to this direction. The detail of the $D(u)$ function provides some evidence for this: Glatter (1979) has shown that two ellipsoids of revolution in contact give rise to two maxima in the $D(u)$ function. Figure 8 in fact shows that whereas the core particle exhibits a single maximum at 4.25 nm, the tetramer particle exhibits two at 4.5 and 6.0 nm. This is best explained if the tetramer particle has a bipartite structure, which can be modeled as two oblate ellipsoids in contact with their major axes parallel.

(*3*) *Circular Dichroism.* CD spectra were obtained for both the tetramer and hexamer particles and are presented in Figure 9. The spectra observed for core particles and 146 bp DNA are in good agreement with those published (Whitlock & Simpson, 1976; Thomas et al., 1977; Olins et al., 1977; Tatchell & Van Holde, 1977; Zama et al., 1978; Bina-Stein, 1978; Weischet et al., 1978; Cowman & Fasman, 1980; Watanabe & Iso, 1981). In the region 260–310 nm the positive DNA band suffers increasing suppression as the amount of histone increases in the following series: 146 bp DNA, tetramer particle, hexamer particle, core particle. Several previous studies (Cowman & Fasman, 1978, 1980; Watanabe & Iso, 1981) have concluded that observed CD spectra in this wavelength range can be accounted for by the linear addition of (1) the spectrum of free DNA and (2) the spectrum of the DNA in core particles. Such a simple linear combination model also suggests itself here, bearing in mind the monotonic change in ellipticity with histone content. What though is the altered DNA conformation in core particles giving rise to the reduced ellipticity? Three explanations exist in the literature: (a) The first explanation is the bending of the DNA in the left-handed supercoil. For the tetramer particle, the neutron scattering results show it to be similar in size and shape to the core particle and therefore to have the same 1.75 superhelical turns of DNA. But the ellipticity of the tetramer at 275 nm is much more positive than that of core particles, and so this explanation can be excluded. (b) The reduced ellipticity in core particles may be due to interactions between the closely spaced gyres of the superhelix (Cowman & Fasman, 1978, 1980). However, Mencke & Rill (1982) have observed suppressed CD spectra in a number of subnucleosomal particles having insufficient DNA to form more than a single supercoil

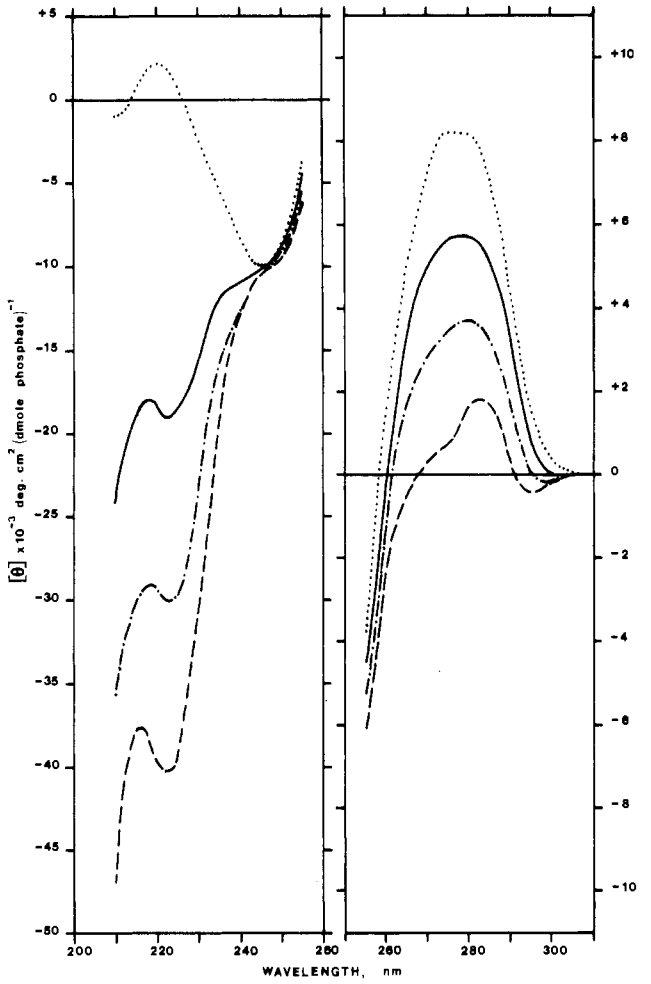

FIGURE 9: Observed CD spectra of core particles (---), $(H3/H4)_2(H2A/H2B)_1$ 146 bp DNA hexamer particles (-·-), $(H3/H4)_2$ 146 bp DNA tetramer particles (—), and the 146 bp DNA (···).

of DNA (of the radius of curvature found in the core particle). (c) The effect is due to changes in the winding angle of the DNA duplex in the direction of the C form as a consequence of histone binding, i.e., an increase in angle between adjacent base pairs and a reduction in the helical repeat (Hanlon et al., 1975; Lawrence et al., 1976). CD studies of superhelical PM2 DNA by Baase & Johnson (1979) relating the ellipticity at 275 nm to the DNA winding angle led to the conclusion that an ellipticity of +1800° means a change in winding angle of +0.71°/bp. Assuming the low ionic strength repeat is 10.6 bp/turn (Rhodes & Klug, 1980), this implies 10.4 bp/turn in the core particle. Nuclease digestion studies have also suggested a reduced repeat in the core particle, even as low as 10.0 bp/turn (Klug & Lutter, 1981). The data in Figure 9 can thus be most simply interpreted as resulting from a linear combination of B-form DNA, i.e., that DNA which has no histone bound to it, and an overwound DNA having bound histone that is in the conformation (assumed uniform) existing in core particles. On this basis the fraction of histone-bound DNA in the tetramer particle is 0.34 (50 bp) and in the hexamer particle is 0.64 (93 bp).

The CD spectrum below 260 nm is due largely to histone. The histone spectra have been approximated by subtracting the spectrum of 146 bp B-form DNA from the total spectrum of core, hexamer, and tetramer particles and converted to units of deg cm^2 (dmol of amino acid)$^{-1}$ for each particle. Histone secondary structure was estimated by curve fitting and also from the ellipticity at 222 nm (see Materials and Methods). Table III gives the results, from which it is seen that little

Table III: Estimated Histone Secondary Structure Content from CD Spectra

particle composition	from θ_{222}, % α-helix	from curve fit			
		% α-helix	% β-sheet	norm[a]	corr[b]
$(H3/H4)_2(H2A/H2B)_2$-(146 bp DNA)$_1$	40.5	43.8	−1.2	0.93	0.96
$(H3/H4)_2(H2A/H2B)_1$-(146 bp DNA)$_1$	40.5	41.1	0.3	1.00	0.95
$(H3/H4)_2$(146 bp DNA)$_1$	40.6	37.7	0.0	1.06	0.98

[a] norm, normalization coefficient [b] corr, correlation coefficient.

β-sheet is present. The value of 44% helix in core octamer protein is close to the values previously reported (Thomas et al., 1977; Weischet et al., 1978; Beaudette et al., 1981). Since protein depletion of the core particle results in only a small change in helicity, it follows that both the $(H2A/H2B)_1$ dimer and the $(H3/H4)_2$ tetramer contain about 40% helix. The small drop in helicity on losing H2A/H2B suggests that the helicity of the $(H2A/H2B)_1$ dimer is slightly greater than that of the $(H3/H4)_2$ tetramer. These helicities are to be compared with values of 44% α-helix and 4% β-sheet for the isolated $(H3/H4)_2$ tetramer and with values of 50% α-helix and 2% β-sheet for the $(H2A/H2B)_1$ dimer, obtained at high ionic strength (Beaudette et al., 1981). It thus appears that changes in secondary structure are not induced when these histone complexes interact with each other and with DNA to form core particles.

(*4*) *Thermal Denaturation.* Melting profiles of core, hexamer, and tetramer particles were obtained in order to assess the length of DNA in each particle which is associated with histone. Figure 10 gives the results plotted as the derivative of the hyperchromicity, dh/dt, vs. the temperature t. The data for core particles is in good agreement with that already published (Tatchell & Van Holde, 1977; Seligy & Poon, 1978; Weischet et al., 1978; Bryan et al., 1979; Cowman & Fasman, 1980). Resolution of the core particle profile into two Gaussian contributions centered at 74 and 60 °C shows that the main transition comprises 67% and the lower melting component 33% of the total hyperchromicity. These figures correspond to 98 and 48 bp of DNA melting in these transitions. In the hexamer particle, the two main transitions are centered at 51.5 and 72.5 °C, but resolution into Gaussian components reveals a small intermediate transition at 63 °C. The lengths of DNA melting in these transitions are 52, 20, and 74 bp (low, middle, and high melting components, respectively). For the tetramer particle the figures are 75, 17, and 54 bp of DNA melting at 44.5, 56.0, and 68.0 °C, respectively. Figure 11 shows a plot of DNA length melting in each transition vs. particle composition (as H2A/H2B dimer content). The DNA lengths melting in the low and middle transitions of tetramer and hexamer particles have been extrapolated to the core particle case. Since the loss of high melting DNA on removal of each H2A/H2B dimer is approximately the same as the increase in the low melting component from hexamer to tetramer (i.e., each "line" shows a slope of 22 bp of DNA per $(H2A/H2B)_1$ dimer), the extrapolation suggests that there is a middle transition of constant magnitude about 19 bp. The broad low melting transition of core particles thus represents two transitions of magnitude 29 and 19 bp. [Some previously published melting profiles of core particles have in fact shown an indication of multiple components in the low melting transition, e.g., Yau et al. (1982)].

What then is the origin of the 29 and 19 bp components in the core particle profile? The presence of the middle transition

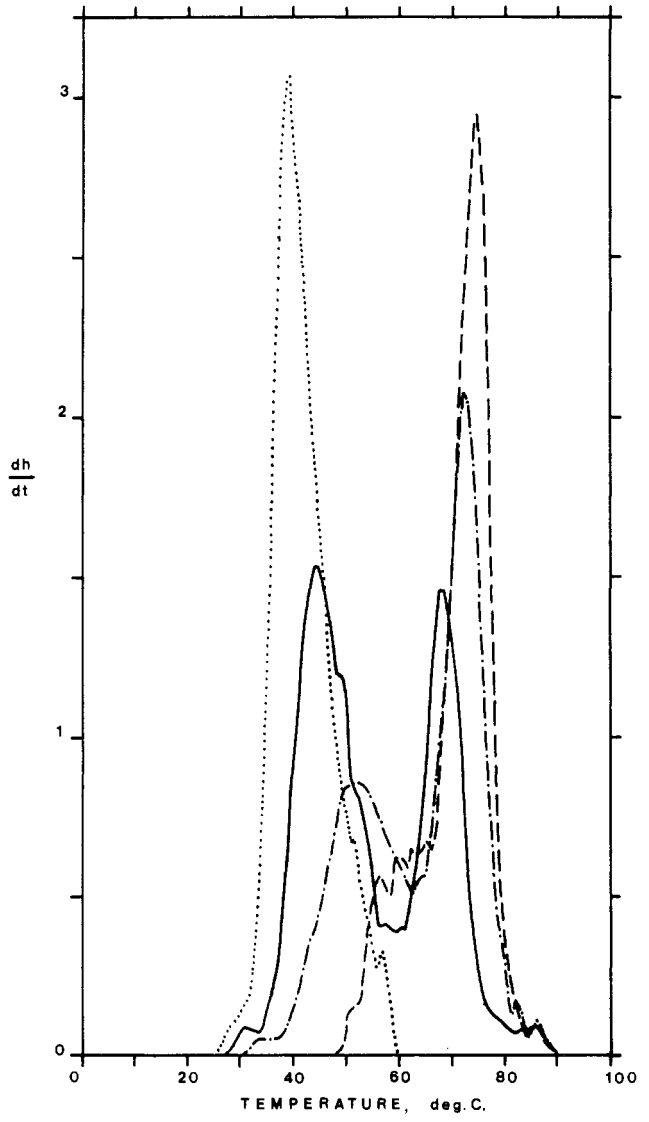

FIGURE 10: First derivative of hyperchromicity with respect to temperature, dh/dt, vs. temperature, t. Plots for core particles (---), $(H3/H4)_2(H2A/H2B)_1$ 146 bp DNA hexamer particles (---), $(H3/H4)_2$ 146 bp DNA tetramer particles (—), and the 146 bp DNA (···).

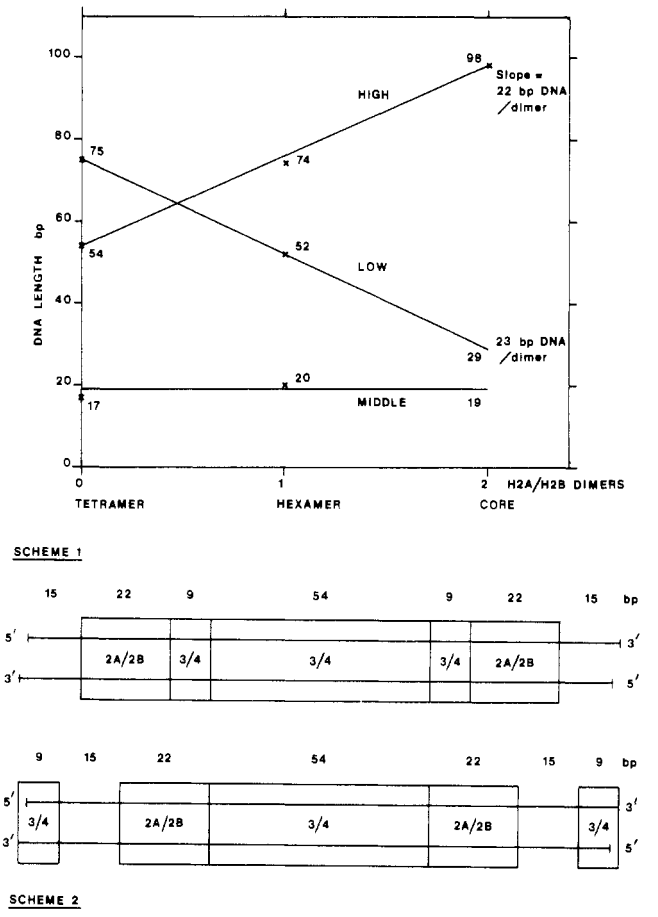

FIGURE 11: (Top) Plot of DNA lengths melting in each of the three transitions (high, middle, and low melting) for core, hexamer, and tetramer particles vs. particle composition. Data taken from Figure 10. (Bottom) Two centrosymmetric schemes of histone binding to 146 bp DNA in the core particle. DNA lengths based on melting data.

in tetramer particles indicates that 19 bp is weakly bound to the H3/H4 histone. The 29 bp is that length of DNA remaining in the low transition when the full complement of core histones is bound and must be due to DNA only weakly bound to histone or even free in the core particle. Weischet et al. (1978) and Simpson (1978) have proposed that the low melting transition of core particles can be assigned to DNA at the ends of the particle. The present analysis thus indicates 15 bp weakly held at both ends of the core particle. Scheme 1 of Figure 11 shows a symmetric histone placing based on this view of 29 bp of terminally located weakly bound (or free) DNA. Since, however, the tetramer is not an expanded particle, the DNA termini are presumably held down by H3/H4 contacts. Scheme 2 shows a symmetric histone arrangement based on this requirement.

(*5*) *Nuclease Digestion.* This approach was adopted in order to obtain information on the relative accessibility of the DNA at different points within the $(H3/H4)_2$ 146 bp DNA particle.

(*a*) *DNase I.* This enzyme digests chromatin and core particles to give a set of bands spaced by about 10.4 nucleotides (Noll, 1974; Prunell et al., 1979). Studies in which DNA was bound to a solid support matrix and then digested (Rhodes & Klug, 1980) showed a 10.6-nucleotide periodicity, and it was concluded that a ladder of bands results from the enzyme being able to approach only from one side of the DNA duplex, the outside in the case of core particles.

A time course DNase I digestion of tetramer particles analyzed on a denaturing DNA gel is shown in Figure 12. At the earliest times, up to about 3 min, a typical ladder of bands is observed, with the obvious exception of a 110-nucleotide band before 1 min. If the tetramer particle contained DNA stretches at its ends that were not supercoiled and therefore extended into free solution and were fully accessible to the enzyme, only a continuum of longer fragments would be produced. The ladder thus implies restricted attack near the ends of the DNA, i.e., fully supercoiled DNA. At later digestion times the larger bands disappear but 70-, 60-, 50-, and 40-nucleotide fragments remain strong, as noted by Stockley & Thomas (1979) for a tetramer particle prepared by a different method. This suggests that the $(H3/H4)_2$ tetramer may be strongly protecting just 70 bp of DNA, leaving about the same length of DNA only weakly protected.

(*b*) *Micrococcal Nuclease.* A time course of digestion of the tetramer particle at 37 °C with this enzyme is shown on a denaturing DNA gel in Figure 13. Digestion at this temperature promotes exonucleolytic trimming of the DNA following initial endonucleolytic cuts and helps to distinguish between histone-bound and histone-free DNA. At the earliest times an approximately 10-nucleotide ladder is seen, superimposed on a strong background and extending down to a

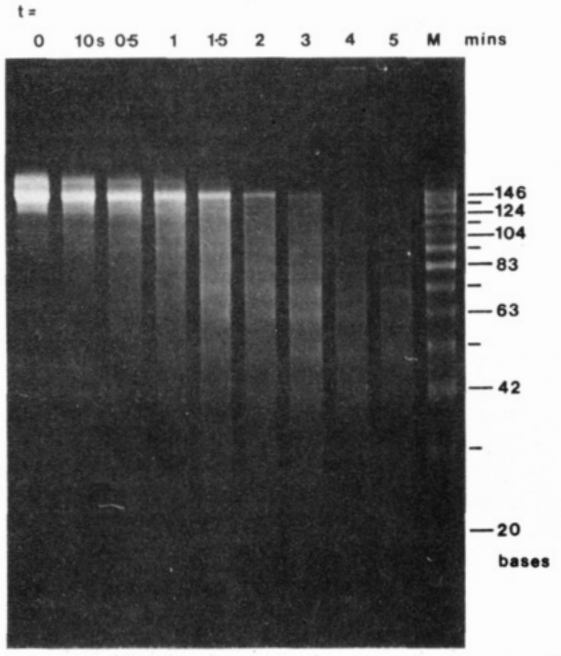

FIGURE 12: Time course of DNase I digestion of $(H3/H4)_2$ 146 bp DNA tetramer particles analyzed by electrophoresis on a 12% polyacrylamide–7 M urea–TBE single-stranded slab gel. M, DNase I digest of core particles.

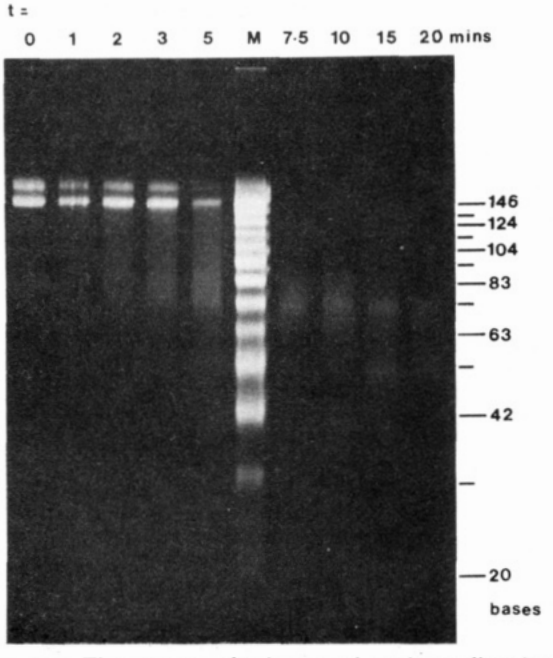

FIGURE 13: Time course of micrococcal nuclease digestion of $(H3/H4)_2$ 146 bp DNA tetramer particles analyzed by single-stranded electrophoresis on a 12% polyacrylamide–7 M urea–TBE slab gel. M, DNase I digest of core particles.

70-nucleotide fragment. Beyond 5 min of digestion this last fragment persists as the main digest product, although 50-nucleotide and weak 60-nucleotide fragments are also seen at later digestion times. The distribution of DNA fragment sizes at the earlier times extends to that of the intact DNA length of the particle before reducing to 70 nucleotides, and this suggests that the histone-free DNA is located primarily at the ends of the particle while the $(H3/H4)_2$ tetramer binds more centrally. The shorter 50- and 60-nucleotide bands can be most readily explained if the enzyme can fairly readily invade the next 10 nucleotides at each end of the protected 70 bp length, beyond which invasion is much slower. The 60-nucleotide band would then be a transient intermediate and the 50-nucleotide band more persistent, as observed.

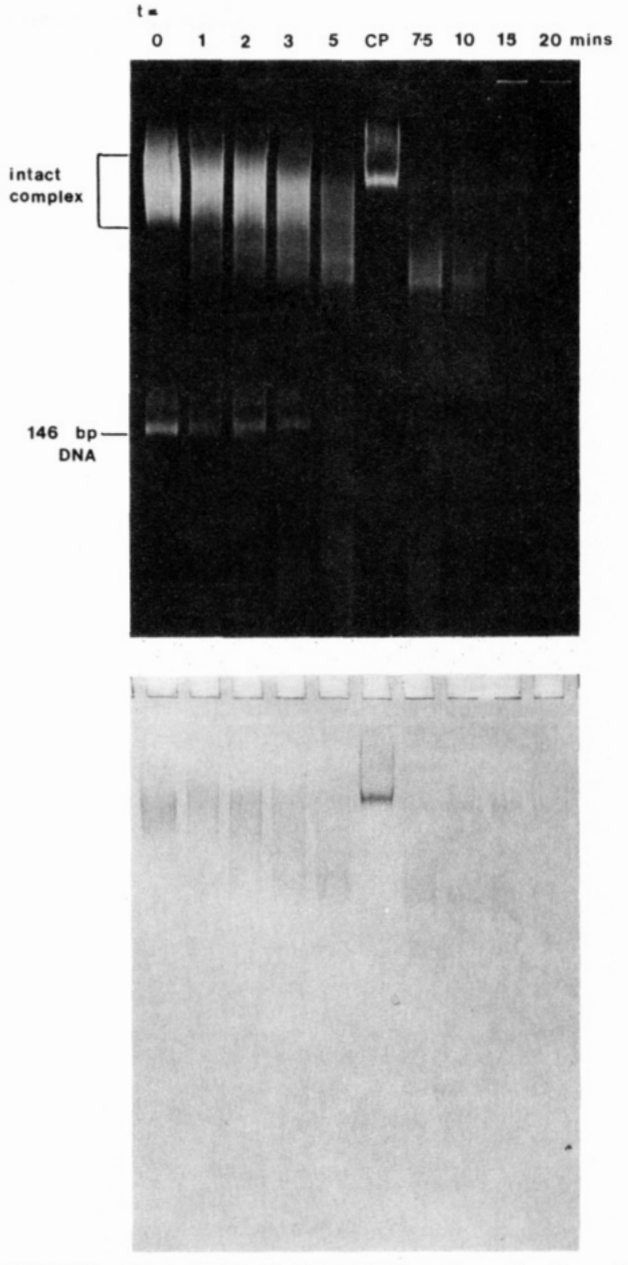

FIGURE 14: Time course of micrococcal nuclease digestion of $(H3/H4)_2$ 146 bp DNA tetramer particles analyzed on a nondenaturing particle gel. Gel stained for DNA with ethidium bromide (top) and then for protein with Coomassie blue (bottom). CP, core particles.

Figure 14 shows a nondenaturing particle gel of the products of the same micrococcal nuclease digestion analyzed in Figure 13. In the ethidium bromide stained gel the broad band of the starting material immediately gives rise to two well-defined products. At 7.5-min of digestion time the slower component is reduced in intensity; a third faster component is also visible, but only the main component is clearly seen in the Coomassie-stained gel. From the DNA gel of Figure 13 the three particles presumably contain 80, 70, and 60 bp DNA, and so the principal product appears to be a particle with the $(H3/H4)_2$ tetramer bound to 70 bp of DNA. An interesting feature of the gel in Figure 14 is the gradual appearance after 7.5-min of digestion of a particle having a mobility only slightly greater than that of core particles. This is at a stage in the digest when there is largely 70 bp DNA and no long-length DNA present. This slowly migrating particle is presumably

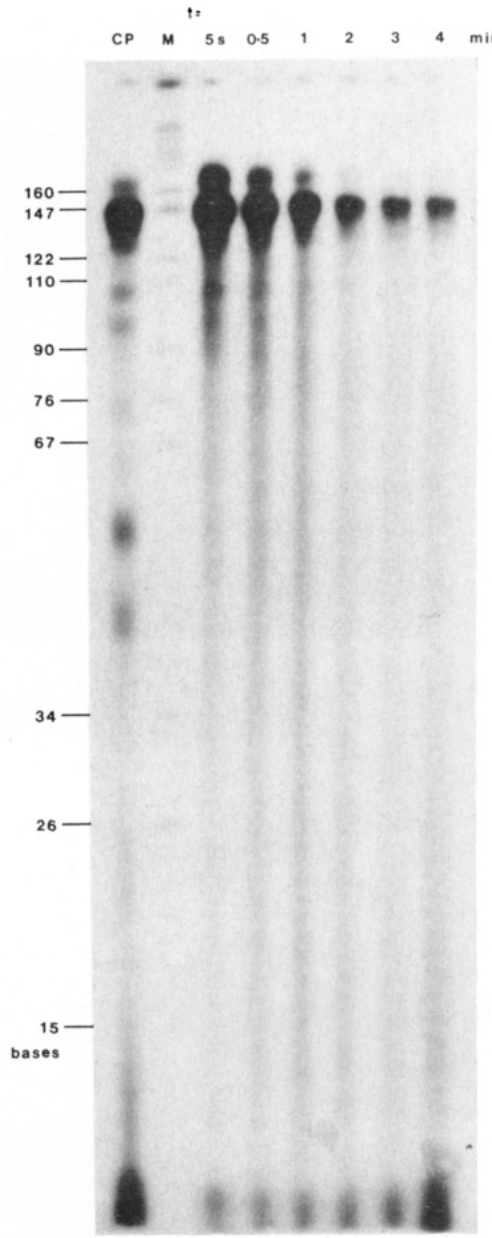

FIGURE 15: Time course of micrococcal nuclease digestion of 5′-end-labeled $(H3/H4)_2$ 146 bp DNA tetramer particles analyzed by electrophoresis on a high-resolution single-stranded gel. CP, DNase I digest of 5′-end-labeled core particles. M, *Hpa*II digest of pBR322 DNA, subsequently 5′ end labeled.

a dimer of the primary product, having a composition 2-[$(H3/H4)_2$ 70 bp DNA]. A particle containing 70 bp of DNA but an octameric histone composition (resulting from histone migration) would have a charge close to zero and could not migrate like a core particle. The ready formation of octameric $(H3/H4)_4$ complexes on core length DNA is well documented, and a previous study of the micrococcal nuclease digestion of H3/H4-reconstituted chromatin (Moss et al., 1977) concluded that the principal product of this reconstitution is in fact a dimer of $(H3/H4)_2$ 65 bp DNA. The nature of this complex has been studied further with H2A/H2B-depleted chromatin (Read & Crane-Robinson, 1985).

(*c*) *Micrococcal Nuclease Digestion of 5′-End-Labeled Tetramer Particles.* The nuclease digestion experiments on unlabeled tetramer particles indicate that 70 bp of DNA is protected but cannot, however, show the location of this protected fragment within the original 146 bp. Figure 15 shows the products of a micrococcal nuclease digest of 5′-end-labeled tetramer particles on a denaturing gel. At the earliest digestion times (5 and 30 s) prominent bands of 129, 107, 96, and 85 nucleotides are seen, the longer two being particularly prominent. The observation of such a strongly modulated pattern of bands indicates that the $(H3/H4)_2$ tetramer does not slide rapidly along the 146 bp length of DNA. Beyond the 1-min digestion time, loss of the 5′ end label due to exonucleolytic action of micrococcal nuclease and secondary cuts more proximal to the 5′ end render the pattern weaker and less specific.

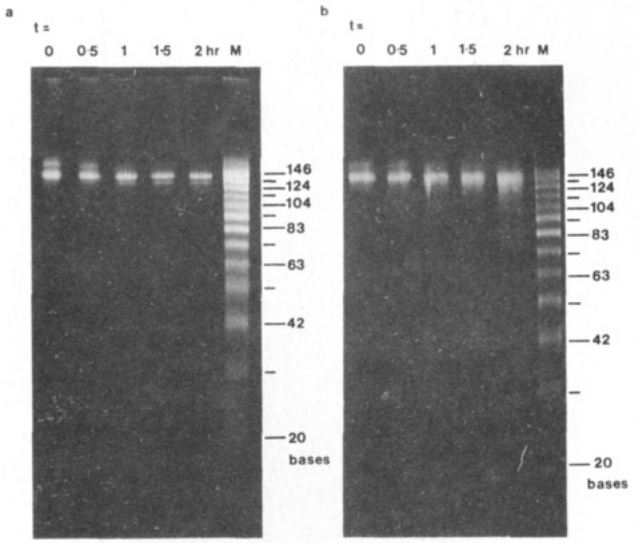

FIGURE 16: Time course of exonuclease III digestion of (a) core particles and (b) $(H3/H4)_2$ 146 bp DNA tetramer particles, analyzed by electrophoresis on a 12% polyacrylamide–7 M urea–TBE slab gel. M, DNase I digest of core particles.

The prominent cut at 107 nucleotides from a 5′ end corresponds to a point 37 nucleotides from the 5′ end of the complementary strand, since S1 nuclease digestion experiments have demonstrated a two-nucleotide overhang in the initial particles (data not shown), assumed to be 3′ protruding (Cockell et al., 1983). The two equivalent sites on each strand are thus 70 bp apart. Primary cutting of the tetramer particle by micrococcal nuclease at symmetrical sites located 70 bp apart suggests that the protected 70-nucleotide fragment seen in both DNase I and micrococcal nuclease digests of unlabeled tetramer particles (Figures 12 and 13) is centrally located.

The fairly prominent fragment in Figure 15 at 96 nucleotides comes from cleavage 11 nucleotides more central than the 107 nucleotide cut. The fragments resulting from the unlabeled micrococcal nuclease digest at longer times included 60- and 50-nucleotide bands that were attributed to 10-nucleotide invasion of both ends of the 70 bp protected region. This would generate the band of 96 nucleotides in the end-labeled products. The weaker band at 85 nucleotides must come from cleavage a further 10 nucleotides inside the protected region.

(*d*) *Exonuclease III.* Previous studies of the action of this enzyme (Riley & Weintraub, 1978; Prunell & Kornberg, 1978) have shown that it can invade, albeit slowly relative to free DNA, the DNA at the ends of core particles. The single-strand products from core particles are characterized by prominent bands at 10.4-nucleotide intervals, indicating that the enzyme is slowed at each turn of the duplex, presumably due to interaction with histones. Exo III might therefore define the size and location of the histone-protected DNA in the tetramer particle. Figure 16 shows a denaturing gel of fragments from Exo III digests of both core and tetramer particles, carried out under identical conditions. Under the conditions

used, the Exo III would degrade histone-free DNA to completion in 1.5 h. After 2 h of digestion a limited invasion of the core particle is seen giving discrete 133- and 122-nucleotide bands. With the tetramer, there is a similar degree of 3′ invasion as judged by the intensity of the remaining 146 bp band, but the products are not of discrete size since a smear is obtained. Two conclusions follow from this: (1) Since the overall rate of 3′ digestion in tetramer particles is similar to that in core particles, the ends of the DNA in the tetramer particle cannot be free and extended into the surrounding solution. This is in accord with the observation of a compact particle using neutron scattering. (2) When 3′ invasion of the tetramer particle does occur (e.g., in the 2-h lane of Figure 16) the enzyme does not pause every 10 nucleotides, as for the core particle. Although there is evidence of a discrete 129-nucleotide fragment, below that is a continuum of products. This implies that in the tetramer particle, unlike the core particle, the DNA immediately beyond the ends is not bound to histone. This therefore suggests a model for the tetramer particle in which about 17 nucleotides at the 3′ ends of the 146 bp DNA are held down by contact with histone, followed by a histone-free region. Digestion with Exo III did not proceed far enough to define the location of the main histone-protected 70 bp region.

Conclusions

The depletion of core particles using 250 mM NaCl and 3–4 M urea in the presence of a cation-exchange resin is capable of yielding preparative quantities of both tetramer $(H3/H4)_2$ 146 bp DNA and hexamer $(H3/H4)_2(H2A/H2B)_1$ 146 bp DNA particles. This procedure is particularly appropriate for further structural and functional studies of these subnucleosomal entities.

In the case of the tetramer particle, the neutron scattering results demonstrate that it is as compact as the core particle. Previous conclusions (Simon et al. 1979; Stockley & Thomas, 1979) that it is in fact an expanded structure were based on the unexpectedly low s value observed, as compared to that of core particles. This low s value, measured here as $s_{20,w}$ = 6.82 S, is confirmed in the present work but is interpreted as a consequence of high solvation, particularly of the DNA. Thomas & Oudet (1979) used the electron microscope to study H3/H4 reconstitutes that, from cross-linking, contained both tetramer and octamer complexes. Both species appeared compact. Appearance on a microscope grid is not necessarily a good guide to solution structure, but the present results indicate that the compact tetramer is not expanded when deposited on grids by the methods used by Thomas & Oudet (1979).

The observation of a broad band in the gel (Figure 4) of the $(H3/H4)_2$ 146 bp DNA particle [also reported by Klevan et al. (1978)] is in contrast to the sharp band from core particles, bearing in mind that the sample studied is compositionally homogeneous and shows no evidence from neutron scattering that the ends of the DNA are even partially extended. Furthermore, the boundary in the ultracentrifuge was not unexpectedly broad. It is possible, however, that the electric field in the gel can induce some partial dissociation of DNA from the tetramer particles. The gel of Figure 14 showing the micrococcal nuclease digest of these particles lends support to this view: if the free 146 bp DNA seen in the gel at $t = 0$ is a contaminant of the particle preparation, it should be digested much more rapidly than the intact particles. Since it is not, we conclude that the 146 bp DNA band results from some complete dissociation of the tetramer particle in the gel. The broad band from $(H3/H4)_2$ 146 bp DNA particles is therefore probably due to partial dissociation of DNA from the ends.

Klevan et al. (1978) concluded that the tetramer particle has an expanded structure on the basis of electric dichroism results. They proposed a model of dimensions 45.0 × 8.0 × 8.0 nm, i.e., with a length ~10% less than that of fully extended 146 bp DNA. This discrepancy might be ascribed to differences in the samples studied. Klevan et al. (1978) did not purify a tetramer particle, so their sample may have contained significant amounts of free 146 bp DNA and the octamer $(H3/H4)_4$ 146 bp DNA particle. The values given by Klevan et al. (1978) for the sedimentation coefficient ($s_{20,w}$ = 6.45 S) and the ellipicity at 282 nm [6888 deg cm^2 (dmol of phosphate)$^{-1}$] both suggest the presence of significant quantities of free DNA in their sample. An alternative explanation, however, for the difference in models is that the electric field used for the dichroism measurements is able to induce a high degree of dissociation of the tetramer particle, well above that seen in particle gels.

Although the full 1.75 superhelical turns of DNA can be maintained by the tetramer $(H3/H4)_2$, both the optical techniques used (CD and melting) and nuclease digestion show that only a limited fraction of the 146 bp of DNA is bound to histone in the tetramer particle. Micrococcal nuclease and DNase I digestion indicate that a centrally located limiting fragment of 70 bp is protected by histones H3/H4, of which 20 bp (2 × 10 bp) is particularly susceptible to further digestion. Optical melting of the tetramer particle (Figure 11) shows that 54 bp are strongly protected by histone (the high melting transition) and a further 17 bp less strongly protected (the middle transition). The DNA lengths protected against nuclease digestion therefore correlate well with the lengths observed in the high and middle melting transitions. End-labeled micrococcal nuclease digestion indicates that the 70 bp of histone-protected DNA are centrally located on the 146 bp of DNA, and this implies a histone binding arrangement like that of Scheme 1 in Figure 11.

The CD results can also give an indication of the amount of DNA bound to histone, on the assumption that the conformational "distortion" of DNA seen by this technique (e.g., overwinding) is uniform along stretches having bound histone; i.e., a two-state model is assumed. If the core particle is taken to be uniformly "distorted" throughout its length, then the tetramer particle contains 50 bp of distorted histone-bound DNA and the hexamer 93 bp as calculated above. If CD distortion in the tetramer particle is induced by the binding of H3 and H4 in only the central "hard to invade" region (50 bp from nuclease digestion), there is good accord between the CD result and nuclease digestion. Addition of a single $(H2A/2B)_1$ dimer to form the hexamer particle is, however, found to distort an extra 43 bp of DNA by the CD criterion, while optical melting shows only 22 bp added to the high melting component. This discrepancy can be partially resolved by first questioning the assumption of 100% CD distortion in the core particle since optical melting shows that 29 bp of DNA denature in the low melting transition of core particles. If these 29 bp do not contribute to the distortion of DNA in the CD spectrum, then only 117 bp (146 − 29) can be regarded as conformationally distorted in the core particle. By use of the ellipticities observed at the peak maxima and linear interpolation between free 146 bp DNA (+8200°) and the core particle (+1800°), it follows that 45 bp are bound to histone in the tetramer particle and 82 bp in the hexamer particle.

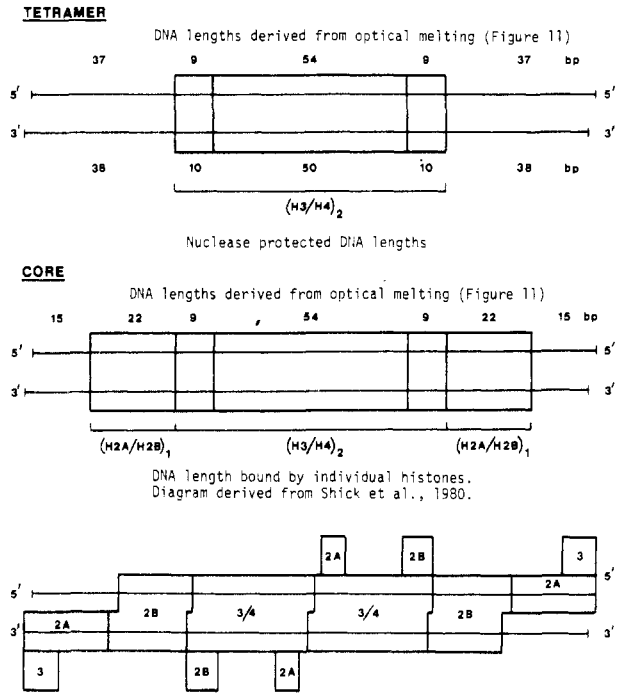

FIGURE 17: Comparison of DNA lengths derived from optical melting and nuclease digestion data for the tetramer particle. Histone/DNA binding arrangement for the core particle that follows from that of the tetramer particle. DNA lengths derived from optical melting. Histone/DNA arrangement in the core particle as proposed from cross-linking data by Shick et al. (1980).

Loss of the first $(H2A/H2B)_1$ dimer thus results in release of 117 − 82 = 35 bp DNA and loss of the second dimer 82 − 45 = 37 bp DNA. Identity of these values is to be expected if the symmetry of the core particle remains in the tetramer particle (as indicated by the central location of H3 and H4 histone in the tetramer). But the melting experiments indicate that only 22 bp of DNA are associated with an $(H2A/H2B)_1$ dimer (Figure 11). If, however, the 10 bp weakly protected by H3/H4 at each end of the central 54 bp (see Scheme 1 of Figure 11) were no longer distorted in the CD spectrum on loss of an $(H2A/H2B)_1$ dimer, then 22 + 10 = 32 bp of DNA would revert to the free DNA conformation. This interpretation of the CD spectra must be regarded as speculative, principally because of the assumptions made as to (1) what constitutes "undistorted" DNA and (2) the uniformity of the distortion on histone binding. In favor of this interpretive scheme is the fact that the same number of base pairs are released from CD distortion on loss of the first and the second $(H2A/H2B)_1$ dimers.

A compact tetramer particle must have the DNA ends bound to histone, and the slow rate of Exo III digestion confirms this. These two terminal contact regions could correspond to the 17 bp observed to melt in the intermediate transition (Scheme 2 of Figure 11), but there is no direct evidence for this assignment; furthermore, Scheme 2 does not explain the protection of 70 bp of DNA in the tetramer particle. Scheme 1 is therefore the histone binding pattern indicated by the present work. Figure 17 shows the DNA lengths bound to histone as derived from optical melting, compared to those lengths protected from nuclease digestion. Figure 17 also shows the histone arrangement in the core particle that follows from this model of the tetramer particle. The DNA lengths bound to each $(H2A/H2B)_1$ dimer (22 bp) come from the optical melting results. The DNA/histone binding regions demonstrated by cross-linking (Shick et al., 1980) are included in Figure 17 and are in good accord with the central 70 bp proposed here for the $(H3/H4)_2$ tetramer location and the flanking 22 bp bound to an $(H2A/H2B)_1$ dimer.

The regions of histone H3 and H4 binding to the DNA can readily be understood on the basis of the recent 0.7-nm core particle structure of Richmond et al. (1984). This shows that the arginine-rich histones are tightly bound to the DNA at sites ±0.5 (H3) and ±3.5 (H4) (where site 0 corresponds to the dyad axis). If the $(H3/H4)_2$ tetramer location is unchanged in the tetramer particle, strong protection of a central 70 bp DNA from nuclease digestion is to be expected. The further trimming of 10 bp of DNA observed for the tetramer particle therefore represents passage through the ±3.5 (H4) contact.

Histone–DNA cross-linking (Schick et al., 1980) and X-ray diffraction (Richmond et al., 1984) of the core particle also indicate that H3 is in contact with the 3′ ends of the core DNA over a region of approximately nine nucleotides. We have no direct evidence for this contact, but as stated above, the compaction of the tetramer particle and the slow Exo III digestion indicate a histone contact in this region. The present results on the tetramer particle therefore show that the binding and positioning of H3 and H4 remain unaltered from that in the core particle of chromatin.

The ability of a single $(H3/H4)_2$ tetramer to organize a full 1.75 superhelical turns of DNA rather than just 1 turn indicates that the primary particle formed by H3 and H4 in the first stages of nucleosome assembly following DNA replication (Worcel et al., 1978; Senshu et al., 1978) is probably as compact as the final core particle. This in turn suggests that histones H2A and H2B play roles very different from H3 and H4; i.e., the H2A/H2B are not primarily involved in maintaining core particle structure but rather in maintaining and perhaps modulating the higher order structure.

The $(H3/H4)_2(H2A/H2B)_1$ 146 bp DNA hexamer particle prepared here has not been studied as fully as the tetramer particle, but from the changes in DNA ellipticity at 275 nm and the optical melting profile, it is intermediate between tetramer and core particles. Since both the tetramer and core particle are of similar overall dimensions, it would be unreasonable to suggest that the hexamer was otherwise, but insufficient material was available for neutron scattering to decide this point definitively. The high *s* value certainly suggests that the hexamer particle is compact. The existence of a stable hexameric particle shows that it could act as an intermediate in the formation of the RNA polymerase II/hexamer complex described by Baer & Rhodes (1983).

ACKNOWLEDGMENTS

We acknowledge Dr. W. B. Gratzer for the use of a CD spectropolarimeter and a UV spectrophotometer for melting studies.

REFERENCES

Baase, W. A., & Johnson, W. C., Jr. (1979) *Nucleic Acids Res. 6*, 797–814.

Baer, B. W., & Rhodes, D. (1983) *Nature (London) 301*, 482–488.

Beaudette, N. V., Fulmer, A. W., Okabayashi, H., & Fasman, G. D. (1981) *Biochemistry 20*, 6526–6535.

Bentley, G. A., Finch, J. T., & Lewit-Bentley, A. (1981) *J. Mol. Biol. 145*, 771–784.

Bina-Stein, M. (1978) *J. Biol. Chem. 253*, 5213–5219.

Bina-Stein, M., & Simpson, R. T. (1977) *Cell (Cambridge, Mass.) 11*, 609–618.

Boseley, P. G., Bradbury, E. M., Butler-Browne, G. S., Carpenter, B. G., & Stephens, R. M. (1976) *Eur. J. Biochem. 62*, 21–31.

Bradbury, E. M., Price, W. C., Wilkinson, G. R., & Zubay, G. (1962) *J. Mol. Biol. 4*, 50–60.

Bryan, P. N., Wright, E. B., & Olins, D. E. (1979) *Nucleic Acids Res. 6*, 1449–1465.

Camerini-Otero, R. D., & Felsenfeld, G. (1977) *Nucleic Acids Res. 4*, 1159–1181.

Camerini-Otero, R. D., Sollner-Webb, B., & Felsenfeld, G. (1976) *Cell (Cambridge, Mass.) 8*, 333–347.

Chen, Y.-H., Yang, J. T., & Chau, K. M. (1974) *Biochemistry 13*, 3350–3359.

Cockell, M., Rhodes, D., & Klug, A. (1983) *J. Mol. Biol. 170*, 423–446.

Cohen, G., & Eisenberg, H. (1968) *Biopolymers 6*, 1077–1100.

Cohn, E. J., & Edsall, J. T. (1943) *Proteins, Amino Acids and Peptides*, Reinhold, New York.

Cowman, M. K., & Fasman, G. D. (1978) *Proc. Natl. Acad. Sci. U.S.A. 75*, 4759–4763.

Cowman, M. K., & Fasman, G. D. (1980) *Biochemistry 19*, 532–541.

Eickbush, T. H., & Moudrianakis, E. N. (1978) *Biochemistry 17*, 4955–4964.

Finch, J. T., Lutter, L. C., Rhodes, D., Brown, R. S., Rushton, B., Levitt, M., & Klug, A. (1977) *Nature (London) 269*, 29–36.

Finch, J. T., Bentley, G. A., Lewit-Bentley, A., Roth, M., & Timmins, P. A. (1980) *Philos. Trans. R. Soc. London, B 290*, 635–638.

Finch, J. T., Brown, R. S., Rhodes, D., Richmond, T., Rushton, B., Lutter, L. C., & Klug, A. (1981) *J. Mol. Biol. 145*, 757–769.

Funding, L., & Steensgaard, J. (1973) MSE (U.K.) Applications Information A8/6/73, 1–19.

Glatter, O. (1979) *J. Appl. Crystallogr. 12*, 166–175.

Godfrey, J. E., Eickbush, T. H., & Moudrianakis, E. N. (1980) *Biochemistry 19*, 1339–1346.

Hanlon, S., Brudno, S., Wu, T. T., & Wolf, B. (1975) *Biochemistry 14*, 1648–1660.

Ibel, K. (1976) *J. Appl. Crystallogr. 9*, 296–309.

Klevan, L., Dattagupta, N., Hogan, M., & Crothers, D. M. (1978) *Biochemistry 17*, 4533–4540.

Klug, A., & Lutter, L. C. (1981) *Nucleic Acids Res. 9*, 4267–4283.

Kornberg, R. D. (1974) *Science (Washington, D.C.) 184*, 868–871.

Laemmli, U. K., & Favre, M. (1973) *J. Mol. Biol. 80*, 575–599.

Lawrence, J. J., Chan, D. C. F., & Piette, L. H. (1976) *Nucleic Acids Res. 3*, 2879–2893.

Lutter, L. C. (1979) *Nucleic Acids Res. 6*, 41–56.

Maniatis, T., Jeffrey, A., & Van de Sande, H. (1975) *Biochemistry 14*, 3787–3794.

Maxam, A. M., & Gilbert, W. (1977) *Proc. Natl. Acad. Sci. U.S.A. 74*, 560–564.

Mencke, A. J., & Rill, R. L. (1982) *Biochemistry 21*, 4362–4370.

Moss, T., Cary, P. D., Abercrombie, B. D., Crane-Robinson, C., & Bradbury, E. M. (1976) *Eur. J. Biochem. 71*, 337–350.

Moss, T., Stephens, R. M., Cary, P. D., Crane-Robinson, C., & Bradbury, E. M. (1977) *Nucleic Acids Res. 4*, 2477–2485.

Noll, M. (1974) *Nucleic Acids Res. 1*, 1573–1578.

Olins, A. L., Carlson, R. D., Wright, E. B., & Olins, D. E. (1976) *Nucleic Acids Res. 3*, 3271–3291.

Olins, D. E., Bryan, P. N., Harrington, R. E., Hill, W. E., & Olins, A. L. (1977) *Nucleic Acids Res. 4*, 1911–1931.

Oudet, P., Germond, J. E., Sures, M., Gallwitz, D., Bellard, M., & Chambon, P. (1978) *Cold Spring Harbor Symp. Quant. Biol. 42*, 287–300.

Pardon, J. F., Worcester, D. L., Wooley, J. C., Tatchell, K., Van Holde, K. E., & Richards, B. M. (1975) *Nucleic Acids Res. 2*, 2163–2176.

Philip, M., Jamaluddin, M., & Chandra, H. S. (1980) *Biochem. Biophys. Acta 42*, 103–108.

Prunell, A., & Kornberg, R. D. (1978) *Cold Spring Harbor Symp. Quant. Biol. 42*, 103–108.

Prunell, A., Kornberg, R. D., Lutter, L. C., Klug, A., Levitt, M., & Crick, F. H. S. (1979) *Science (Washington, D.C.) 204*, 855–858.

Read, C. M., & Crane-Robinson, C. (1985) *Eur. J. Biochem.* (in press).

Rhodes, D., & Klug, A. (1980) *Nature (London) 286*, 573–578.

Richmond, T. J., Finch, J. T., Rushton, B., Rhodes, D., & Klug, A. (1984) *Nature (London) 311*, 532–537.

Riley, D., & Weintraub, H. (1978) *Cell (Cambridge, Mass.) 12*, 281–293.

Ruiz-Carrillo, A., & Jorcano, J. L. (1979) *Biochemistry 18*, 760–768.

Schmatz, W., Springer, T., Schelton, J., & Ibel, K. (1974) *J. Appl. Crystallogr. 7*, 96–116.

Seligy, V. L., & Poon, N. H. (1978) *Nucleic Acids Res. 5*, 2233–2252.

Senshu, T., Fukuda, M., & Ohashi, M. (1978) *J. Biochem. (Tokyo) 84*, 985–988.

Schick, V. V., Belyavsky, A. V., Bavykin, S. G., & Mirzabekov, A. D. (1980) *J. Mol. Biol. 139*, 491–517.

Sibbet, G. J., & Carpenter, B. G. (1983) *Biochim. Biophys. Acta 740*, 331–338.

Simon, R. H., Camerini-Otero, R. D., & Felsenfeld, G. (1978) *Nucleic Acids Res. 5*, 4805–4818.

Simpson, R. T. (1979) *J. Biol. Chem. 254*, 10123–10127.

Sollner-Webb, B., Camerini-Otero, R. D., & Felsenfeld, G. (1976) *Cell (Cambridge, Mass.) 9*, 179–193.

Sollner-Webb, B., Melchior, W., & Felsenfeld, G. (1978) *Cell (Cambridge, Mass.) 14*, 611–627.

Stein, A. (1979) *J. Mol. Biol. 130*, 103–134.

Stockley, P. G., & Thomas, J. O. (1979) *FEBS Lett. 99*, 129–135.

Suau, P., Kneale, G. G., Braddock, G. W., Baldwin, J. P., & Bradbury, E. M. (1977) *Nucleic Acids Res. 4*, 3769–3786.

Tetchell, K., & Van Holde, K. E. (1977) *Biochemistry 16*, 5295–5303.

Thomas, G. J., Prescott, B., & Olins, D. E. (1977) *Science (Washington, D.C.) 197*, 385–388.

Thomas, J. O., & Kornberg, R. D. (1975a) *Proc. Natl. Acad. Sci. U.S.A. 72*, 2626–2630.

Thomas, J. O., & Kornberg, R. D. (1975b) *FEBS Lett. 58*, 353–358.

Thomas, J. O., & Kornberg, R. D. (1978) *Methods Cell Biol. 18*, 429–440.

Thomas, J. O., & Oudet, P. (1979) *Nucleic Acids Res. 7*, 611–623.

Watanabe, K., & Iso, K. (1981) *J. Mol. Biol. 151*, 143-163.
Weber, K., & Osborn, M. (1969) *J. Biol. Chem. 244*, 4406-4412.
Weischet, W. O., Tatchell, K., Van Holde, K. E., & Klump, H. (1978) *Nucleic Acids Res. 5*, 139-160.
Whitlock, J. P., & Simpson, R. T. (1976) *Nucleic Acids Res. 3*, 2255-2266.
Worcel, A., Han, S., & Wong, M. L. (1978) *Cell (Cambridge, Mass.) 15*, 969-977.
Yau, P., Thorne, A. W., Imai, B. S., Matthews, H. R., & Bradbury, E. M. (1982) *Eur. J. Biochem. 129*, 281-288.
Zama, M., Bryan, P. N., Harrington, R. E., Olins, A. L., & Olins, D. E. (1978) *Cold Spring Harbor Symp. Quant. Biol. 42*, 31-41.

Distribution of Apolipoprotein A-I, C-II, C-III, and E mRNA in Fetal Human Tissues. Time-Dependent Induction of Apolipoprotein E mRNA by Cultures of Human Monocyte-Macrophages†

Vassilis I. Zannis,*,‡,§ F. Session Cole,§ Cynthia L. Jackson,§ David M. Kurnit,§ and Sotirios K. Karathanasis§

Section of Molecular Genetics, Cardiovascular Institute, Departments of Medicine and Biochemistry, Boston University Medical School, Boston, Massachusetts 02118, and Children's Hospital, Boston, Massachusetts 02115

Received December 7, 1984

ABSTRACT: Recently developed molecular probes for human apolipoprotein (apo) genes have been used to study the specificity of human tissue expression of the apo A-I, apo C-II, apo C-III, and apo E genes. We have found that apo E mRNA was present in all tissues examined. On the basis of total RNA concentration the relative abundance of apo E mRNA expressed as a percentage of the liver value is as follows: adrenal gland and macrophages, 74-100%; gonads and kidney, 12-15%; spleen, brain, thymus, ovaries, intestine, and pancreas, 3-9%; heart, 1.5%; stomach, striated muscle, and lung, <1%. The relative concentration of apo E mRNA in cultures of human peripheral blood monocyte-macrophages increases dramatically as a function of time in culture, and after 5 days, it compares to that of liver. The human tissues shown to synthesize apo E mRNA were also examined for their ability to synthesize apo A-I, apo C-II, and apo C-III mRNA. The relative abundance of apo A-I, apo C-III, and apo C-II mRNA expressed as a percentage of the liver value is as follows: apo A-I, intestine, 50%; apo A-I, pancreas and gonads, 12%; apo A-I, kidney, 4%; apo A-I, adrenal, 2.5%; apo A-I, ovaries and heart, 1%; apo A-I, stomach and thymus, <1%; apo C-III, intestine, 62%; apo C-III, pancreas, 7%; apo C-II, intestine, 3%; apo C-II, pancreas, <1%. The knowledge of tissue specificities in the synthesis of apolipoproteins is important for our understanding of the regulation of apolipoproteins and lipoprotein metabolism.

The definition of the sites of apolipoprotein synthesis has been the subject of extensive investigation during the last five years. On the basis of protein quantitation techniques, two organs in mammalian species, the liver and the intestine, were thought to produce most of the plasma apolipoproteins (Windmueller et al., 1973; Marsh, 1976; Hamilton et al., 1976; Glickman & Green, 1977; Green et al., 1978; Schonfeld et al., 1978; Wu & Windmueller, 1979; Windmueller & Wu, 1981). Recently, other tissues have been shown to synthesize some of the apolipoproteins (Blue et al., 1980, 1982, 1983; Basu et al., 1982). The development of probes for the human apolipoprotein genes (Breslow et al., 1982a,b, 1983; Karathanasis et al., 1985; Zannis et al., 1984; Jackson et al., 1984) permits a qualitative and quantitative comparison of the amounts of specific apolipoprotein mRNA present in different tissues. These studies show that multiple human tissues synthesize apo A-I, apo C-II, apo C-III, and apo E mRNA and that the synthesis of some of the mRNAs is tissue specific.

Experimental Procedures

Materials. Radiolabeled nucleotides [α-^{32}P]dATP, [α-^{32}P]dCTP, [α-^{32}P]dGTP, and [α-^{32}P]TTP were purchased from New England Nuclear. The Klenow fragment of DNA polymerase I and the M13 sequencing primer were purchased from New England Biolabs. DNase I was purchased from Sigma, and agarose and Bio-Gel P-60 were obtained from Bio-Rad. Nitrocellulose filters were obtained from Schleicher & Schuell, Inc. Medium 199 was purchased from M. A. Bioproducts.

Cell Cultures. Primary monolayer cultures of adherent human peripheral blood monocytes were established and maintained by using a modification of the method of Einstein et al. (1976). Briefly, peripheral blood leukocytes were isolated from ethylenediaminetetraacetic acid (EDTA) anticoagulated blood of adult human subjects by dextran sedimentation, washed, and incubated overnight at 4 °C to decrease adherence of polymorphonuclear leukocytes and lymphocytes. Mono-

† This work was supported by grants from the National Institutes of Health (HL33952, HL32032, and HD00584), the March of Dimes Birth Defects Foundation (1-817), and the American Heart Association (83-963). V.I.Z. is an Established Investigator of the American Heart Association.

* Address correspondence to this author at Boston University Medical School.
‡ Boston University Medical School.
§ Children's Hospital.

0006-2960/85/0424-4450$01.50/0